筑　波　大　学

博 士 （医 学） 学 位 論 文

Role of Glycoprotein NMB in Carcinogenesis of Laryngeal Squamous Cell Carcinoma

（喉頭扁平上皮がんにおける Glycoprotein NMBの作用）

２０２２

筑波大学大学院博士課程人間総合科学研究科

Lev Manevich

ABSTRACT

[Purpose]

Laryngeal Squamous Cell Carcinoma (LSCC) is the second common cancer of the respiratory tract and is one of the major representatives of head and neck SCC (HNSCC). The incidence rate is among twenty most frequent cancers worldwide in 2020. The main reasons of the cancer frequency, treatment resistance, tumor relapse, and sore consequences for patients are difficulties of early diagnosis, ubiquitous utilization of platinum-based drugs, and radical surgical solutions. Glycoprotein NMB (GPNMB) is a crucial mediator of carcinogenesis in versatile cancer origins, including some representatives of HNSCC. To improve diagnosis and treatment, the novel marker and a therapeutic target for LSCC are awaited, and GPNMB is one of the promising candidates. Hence, my aim is to figure out the function and importance of the GPNMB in LSCC progression.

[Materials and methods]

In the following study, to examine the presence of GPNMB and other targets in HNSCC and LSCC, I used Western blot (WB), reverse transcription polymerase chain reaction (RT-PCR), quantitative real time PCR (qRT-PCR), RNA-sequencing among cell lines derived from the malignant lesions of LSCC. I analyzed messenger RNA expression patterns from publicly available The Cancer Genome Atlas (TCGA), based on comparison between the HNSCC patients vs. non-malignant cases. Immunohistochemistry and immunofluorescence (IHC, IF) were performed with formalin-fixed, paraffin-embedded (FFPE) sections of tumors from

xenograft models and tissues of LSCC patients cohort. I have implemented enzyme-linked immunoassay (ELISA) to measure cleaved soluble GPNMB (sGPNMB) concentrations in serum samples of LSCC patients vs. non-malignant control. To elucidate the physiological function and molecular mechanism of GPNMB in LSCC progression, I implemented knockdown (KD) technique by establishing lentivirus-mediated transduction system with constructed plasmids carrying small hairpin RNA (shRNA) targeting GPNMB messenger RNA (mRNA); transfection reagent-mediated transduction system including small interfering RNA (siRNA) targeting defensin beta 4A (DEFB4A). For further investigation I used next assays: cell proliferation (MTS assay), wound-healing scratch migration, 3D sphere formation, and *in vivo* tumor formation by subcutaneous injection of laryngeal SCC cell lines in BALB/cAJcl-*nu/nu* mice.

[Results]

GPNMB mRNA and protein were abundantly and diversly expressed among LSCC-derived cell lines and among HNSCC patients cohort from TCGA database with significantly higher levels compared to control non-malignant groups. Similar patterns were observed in data from IHC/IF staining of LSCC specimens with undetectable expression of GPNMB in normal squamous tissues, while there was no significant difference in serum levels of sGPNMB between groups of LSCC-patients and non-malignant control, assessed by ELISA. Physiologically, GPNMB silencing significantly hindered cellular proliferation in monolayer cultures, 3D sphere formation, and wound-healing migration of two examined LSCC cell lines. Furthermore, tumor formation *in vivo* was significantly abrogated from GPNMB KD cells. Our data shows GPNMB silencing in LSCC cell lines has dramatically altered the expression of genes from various

pathways, including major suppression of cellular proliferation, cellular migration, and lymphovascular-invasion-related (LVI) genes. Interestingly, according to IHC/IF data obtained from xenograft models and clinical specimens, GPNMB and Ki-67 (proliferation marker) were mutually inversely expressed in tissues, suggesting the non-proliferative, quiescent nature of cells with GPNMB expression; however, the qRT-PCR analysis in GPNMB KD cells revealed significant expression reduction in one out of nine cancer stem cells (CSCs) related markers, which was *BMI1*. Finally, GPNMB KD overexpressed DEFB4A in LSCC cells, while the subsequent KD of DEFB4A could significantly recover sphere formation in one out of two tested cell-lines.

[Discussion]

These results showed hindered cellular migration in 2D, sphere formation in 3D, and tumor formation in xenograft models of LSCC cell lines during the silencing of GPNMB, which are similar outcomes as in previously reported studies in breast cancer or oral SCC. In comparison with our previous experiments on breast cancer cell lines, where proliferation was affected by GPNMB KD, this study shows depletion of GPNMB reduced the proliferation ability of LSCC cell lines in 2D. Plenty of oncogenes were affected by GPNMB silencing, including downregulation of *TGFB2* and upregulation of *DAB2*, which leads to better overall survival (OS) prognosis in HNSCC patients. As upregulation of IL6 and of other LVI-related genes leads to advancement and metastatic feature of LSCC, GPNMB KD could abrogate those expressions, suggesting that GPNMB is responsible for metastatic phenotype in LSCC. Findings of mutual inverse correlation between GPNMB and Ki-67 expressions in tissues suggest the non-

proliferative, quiescent nature of cells with GPNMB expression, which recently is considered to be a link to cancer stem cell phenotype. However, further study of GPNMB involvement in CSCs populations in LSCC is required, as in this study there was only one consistent significant decrease among both GPNMB KD LSCC cell lines in *BMI1* expression. Finally, GPNMB KD significantly upregulated the expression of *DEFB4A*, a target gene of NF-κB pathway, in both laryngeal cell lines, while the siRNA KD of DEFB4A significantly recovered the sphere forming ability of a cell line, derived from advanced LSCC origin.

[Conclusion]

Since there are few reports on the GPNMB involvement in HNSCC present up to date, my work shows the importance of GPNMB functionality and correlation within LSCC progression, suggesting its involvement in regulation of CSCs population and partially discovers a novel mechanism of GPNMB – DEFB4A axis. As such, I suggest GPNMB as a diagnostic marker for surgically obtained specimens and as a novel therapeutic target within LSCC patients.

ABBREVIATION LIST

AKT: Protein Kinase B

ALDH1A1: Aldehyde Dehydrogenase 1 Family Member A1

APC: Antigen Presenting Cell

ATCC: American Type Culture Collection

BMI1: B Lymphoma Mo-MLV Insertion Region 1 Homolog

CSC: Cancer Stem Cell

CT: Chemotherapy

DAB2: Disable Homolog 2

DAPI: 4′,6-diamidino-2-phenylindole

DC-HIL: Dendritic Cell-associated HSPG-dependent Integrin Ligand

DEFB4A: Defensin Beta 4A

DEG: Differentially Expressed Gene

DLM: Dileucine Motif

DMEM: Dulbecco's Modified Eagle's Medium

ECD: Extracellular Domain

EGFR: Epidermal Growth Factor Receptor

ELISA: Enzyme-linked Immunoassay

EMT: Epithelial-mesenchymal Transition

ERK: Extracellular Signal-regulated Kinase

FBS: Fetal Bovine Serum

FDR (p-value): False Discovery Rates

FFPE: Formalin-Fixed, Paraffin-Embedded

GAPDH: Glyceraldehyde-3-Phosphate Dehydrogenase

GLI1: Glioma-associated Oncogene Homolog 1

GLOBOCAN: Global Cancer Incidence, Mortality and Prevalence

GPNMB: Glycoprotein NMB

GSEA: Gene Set Enrichment Analysis

HD: Heterodimerization Domain

HEK 293T: Human Embryonic Kidney 293T cell line

HNSCC: Head & Neck Squamous Cell Carcinoma

HPV: Human Papilloma Virus

HRP: Horseradish Peroxidase

ICD: Intracellular Domain

IF: Immunofluorescence

IHC: Immunohistochemistry

IL6: Interleukin 6

JAK: Janus Kinase

KD: Knockdown

KLD: Kringle-like Domain

KLF4: Kruppel-like factor 4

Ki-67: Marker of Proliferation Ki-67

LB medium: Lysogeny Broth Medium

LSCC: Laryngeal Squamous Cell Carcinoma

LVI: Lymphovascular Invasion

M-WD: Moderately to Well Differentiated

MAPK, MEK: Mitogen-activated Protein Kinase

MITF: Microphthalmia-associated Transcription Factor

MMP: Matrix Metalloproteinase

MSI1: Musashi1

MTS assay: 3-(4,5-dimethylthiazol-2-yl)-5-(3-carboxymethoxyphenyl)-2-(4-sulfophenyl)-2H tetrazolium) Assay

MWD: Moderately Well Differentiated

NF-κB: Nuclear Factor Kappa B

NOTCH1: Notch Homolog 1, Translocation-Associated

NTRK: Neurotrophic Tyrosine Receptor Kinase

OA: Osteoactivin

OE: Overexpression

OSCC: Oral Squamous Cell Carcinoma

PD: Poorly Differentiated

PEI: Polyethyleneimine

PI3K: Phosphatidylinositol 3-kinase

PKD: Polycystic Kidney Disease Homology Domain

PMEL17: melanocyte-specific glycoprotein Pmel17

POU5F1 (OCT-4): POU Class 5 Homeobox 1

PROM1 (CD133): Prominin1

PVDF: Polyvinylidene Difluoride

RGD: Integrin Recognition Domain

RIN: RNA Integrity Number

RT-PCR: Reverse Transcription Polymerase Chain Reaction

RT: Radiation Therapy

Raf: Rapidly Accelerated Fibrosarcoma

Ras: Rat Sarcoma Virus

SD: Standard Deviation

SDS: Sodium Dodecyl Sulfate–Polyacrylamide

SOX2: Sex Determining Region Y-box 2

SP: Signal Peptide

SPF: Specific Pathogen Free

STAT3: Signal Transducer and Activator of Transcription 3

TBST: Tris-buffered Saline with Tween® 20

TCGA: The Cancer Genome Atlas

TGFβ2: Transforming Growth Factor Beta 2

TMD: Transmembrane Domain

TNBC: Triple-negative Breast Cancer

TPM: Transcripts Per Kilobase Million

TRP1: Tyrosinase-related Protein 1

TYR: Tyrosinase

UMSCC: University of Michigan Squamous Cell Carcinoma Cell Line

WB: Western Blotting

WD: Well Differentiated

bFGF: Basic Fibroblast Growth Factor

hem-ITAM: Half Immunoreceptor Tyrosine-based Activation Motif

mRNA: Messenger RNA

mTOR: Mammalian Target of Rapamycin

qRT-PCR: Quantitative Real Time Polymerase Chain Reaction

rhOA: Recombinant Osteoactivin

sGPNMB: Soluble Glycoprotein NMB

shRNA: Short Hairpin RNA

siRNA: Small Interfering RNA

TABLE OF CONTENTS

Abstract

Abbreviation list

Table of contents

Chapter 1. Introduction…….....1

1.1. Laryngeal Squamous Cell Carcinoma…….……..1

1.1.1. The incidence of Laryngeal Squamous Cell Carcinoma…….…...1

1.1.2. Molecular landscape in LSCC…….……2

1.1.3. Chemical and target therapies in LSCC…….3

1.2. Glycoprotein nmb…….……...4

1.2.1. Outline of GPNMB…….……..4

1.2.2. GPNMB in HNSCC……..6

1.3. Cancer Stemness……..7

Chapter 2. Materials and Methods…….…..9

2.1. Cells and cell cultivation…….....9

2.2. Construction of DNA-plasmids for short hairpin-mediated knockdown…..…..11

2.3. Knockdown using lentiviral system…….....12

2.4. Western blotting……12

2.5. Reverse transcription and quantitative PCR analysis……...15

2.6. Proliferation assay in 2D……..16

2.7. Tumor sphere formation assay…….……...17

2.8. Wound-healing scratch assay……..17

2.9. Analysis of mRNA sequencing ……....17

2.10. Analysis of RNA-sequencing results…….18

2.11. Formation of tumors *in vivo* …….....19

2.12. LSCC patients and tissue specimens ……19

2.13. Immunohistochemical and immunofluorescence staining …….20

2.14. ELISA sandwich assay……...20

2.15. Statistical analysis……..….21

Chapter 3. Results…….…...22

3.1. GPNMB is highly expressed in HNSCC and LSCC…….….22

3.2. GPNMB silencing impairs cellular proliferation, sphere formation, and cellular migration of LSCC cell lines……...22

3.3. GPNMB silencing downregulates cellular proliferation, migration, and lymphovascular-invasion-related genes…….23

3.4. GPNMB silencing impairs tumor formation of LSCC cell lines *in vivo*……..24

3.5. The effect of GPNMB KD on CSCs markers in LSCC cell lines……..……25

3.6. GPNMB is expressed in malignant lesions of LSCC patients…….……..25

3.7. Soluble GPNMB in LSCC patients and non-malignant cohort……..……..26

3.8. GPNMB knockdown-mediated DEFB4A upregulation leads to suppression of sphere formation in UMSCC-11B……..27

Chapter 4. Discussion……..53

Chapter 5. Conclusion…….58

Chapter 6. Graphical Summary…….60

References…….61

Acknowledgements……..80

CHAPTER 1. INTRODUCTION

1.1. Laryngeal Squamous Cell Carcinoma

1.1.1. The incidence of Laryngeal Squamous Cell Carcinoma

Laryngeal Squamous Cell Carcinoma (LSCC) is the second most common representative of respiratory tract tumors and one of the most common representatives of Head and Neck Squamous Cell Carcinoma (HNSCC) (Steuer et al., 2017). SCC occurrence in larynx is more frequent in male population (5.8 patients per 100,000), while also being present in women (1.2 patients per 100,000) (Baselga, 2002). The worldwide incidence rates of LSCC in 2020 was 160,265 and 24,350 cases among male and female patients respectively (Ferlay et al., 2021) (Figure 1.1.1). Whereas the survival rate of other representatives within HNSCC has increased, LSCC survival was either decreased (Siegel et al., 2016) or remained static (Pulte & Brenner, 2010) with mortality in 2020 being 85,351 and 14,489 deaths among men and women respectively (Ferlay et al., 2021). Several complications, as advancement and propagation through lymphovascular invasion (LVI) (Zhang et al., 2020), metastasis or frequent relapse define the poor progression of LSCC (Johnson et al., 2020). Among main independent risk factors, underlying the increase of the LSCC incidence by 10 - 30 times, are alcohol and tobacco consumption (Kuper et al., 2002; Talamini et al., 2002). The occupational exposure to such environmental factors as textile particles or asbestos were also reported as risks of LSCC occurrence (Paget-Bailly et al., 2012).

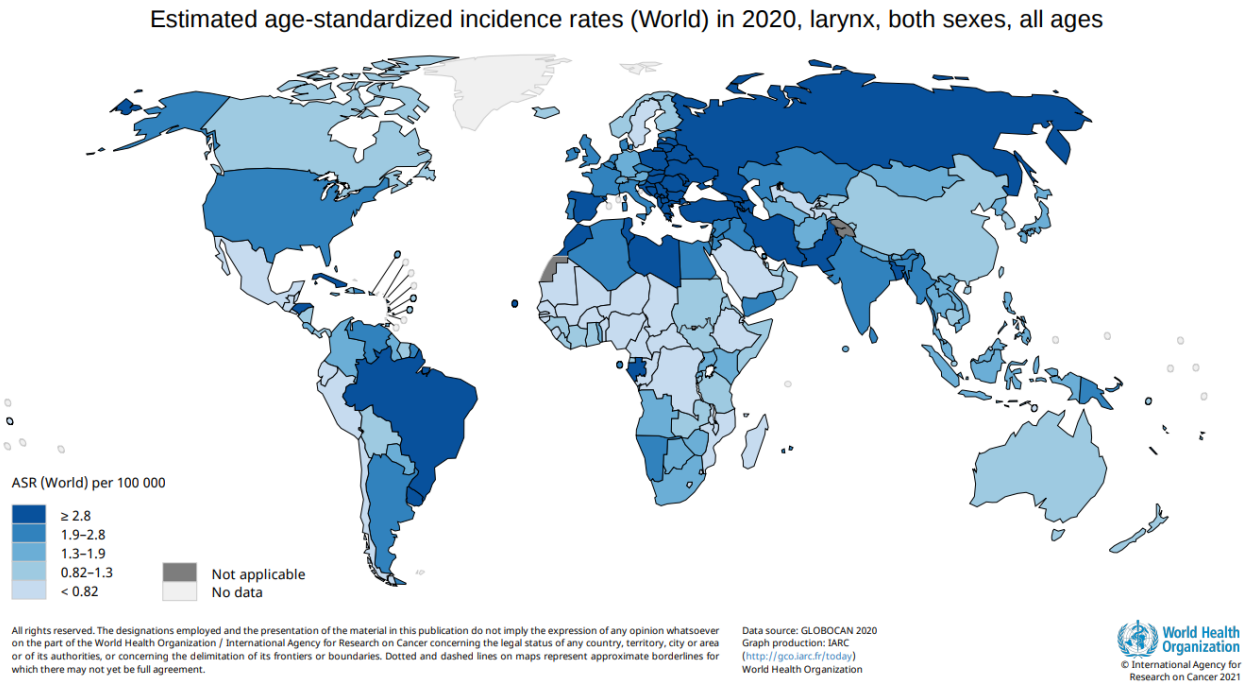

Figure 1.1.1. Estimated LSCC incidence rates worldwide. GLOBOCAN 2020, Ferlay et al.

1.1.2. Molecular landscape in LSCC

Up until recently among plethora of revealed oncogenic pathways in HNSCC and in LSCC, several have shown a prominent effect on carcinoma progression. One of those candidates are EGFR-related downstream targets. Ligand-mediated activation and autophosphorylation of EGF receptor result in stimulation of its pathway – Ras/Raf/MEK/ERK within MAPK axis, PI3K/AKT pathway, and JAK/STAT3 downstream, which are reported to have an oncogenic role in HNSCC, decreasing the overall survival (OS) (Kalyankrishna & Grandis, 2006; Leemans et al., 2011). Other studies revealed the importance of alterations in NOTCH signaling. With HNSCC progression, consistent accumulation of mutations occurs primarily in NOTCH1, resulting in duality of functioning (Fukusumi & Califano, 2018). Normally, it acts as a tumor suppressor in HNSCC (Dotto, 2008), and while most mutations occur in extracellular domain (ECD) of NOTCH1 and

decrease the affinity of ligand binding (Agrawal et al., 2011; Perdomo et al., 2018; Rivelli et al., 2014), that results in NOTCH1 loss of function and further HNSCC progression (Shah et al., 2020; Stransky et al., 2011). Other reports suggest mutations occurring in heterodimerization domain (HD) of NOTCH1 lead to its activation and a further crosstalk with PI3K and STAT3, resulting in HNSCC progression (Fattizzo et al., 2020; Shah et al., 2020). As the mutation pattern of head and neck SCC is heterogenous with possible explicit changes within a gene, NOTCH1 therapeutic targeting remains inconclusive (Shah et al., 2020). Other abnormalities include mutations in p53 (Bradford et al., 1997; Poeta et al., 2007) or constitutively upregulated STAT3 (Geiger et al., 2016; Sun et al., 2018).

1.1.3. Chemical and target therapies in LSCC

Towards the end of 20th century total laryngectomy was one of the most frequent solutions for treatment of advanced LSCC cases, however several decades ago platinum-based chemotherapy (CT), and later radiation therapy (RT), have become a golden standard of non-surgical treatment up until nowadays (Department of Veterans Affairs Laryngeal Cancer Study Group et al., 1991; Zhang et al., 2019). Despite the advantages of CT over the surgical approach alone (Cooper et al., 2004; Machiels et al., 2020), acquisition of chemoresistance, induced dormancy with further relapse, and severe side effects are persistent common disadvantages occurring in patients (Forastiere et al., 2003; Rivelli et al., 2015). To improve the non-surgical methods of LSCC treatment, several studies aimed to find a potential target for precise therapy. They have confirmed the relevance of high expression of the epidermal growth factor receptor (EGFR) in HNSCC and in LSCC in particular (Kontić et al., 2015; Kriegs et al., 2019). While phosphorylated EGFR activates downstream oncogenic pathways through AKT, MAPK and STAT (Leemans et al., 2011),

such EGFR inhibitors, as cetuximab, abrogate the EGFR functionality and result in better prognosis within advanced, metastatic, or recurrent cases (Herchenhorn & Ferreira, 2011; Specenier & Vermorken, 2011). Nonetheless, monotherapy with EGFR-inhibitors resulted in mediocre positive outcomes due to the heterogeneous feature of LSCC, mutations in EGF receptor, and other resistant mechanisms (Braig et al., 2017; Lefebvre et al., 2013; Magrini et al., 2016). Despite that fact, more enhanced OS was achieved by utilizing the combination of anti-EGFR treatment and CT/RT comparing to the solitary utilization of those medical applications, as well as more prominent existence of side effects within combined treatment (Alsahafi et al., 2019; Burtness et al., 2005; Vermorken et al., 2008). This confirms the need for further discovery of alternative novel targets to increase optimistic treatment outcomes.

1.2. Glycoprotein nmb

1.2.1. Outline of GPNMB

Glycoprotein nmb (GPNMB) with another name as Osteoactivin (OA), is a type 1 transmembrane protein. Generally, the structure is divided into three domains: extracellular (ECD), transmembrane (TMD), and intracellular (ICD) (Maric et al., 2013) (Figure 1.2.1). Recently our laboratory performed intramolecular studies. One of those revealed the importance of the kringle-like domain (KLD), which is a part of ECD, in tumorigenesis of breast cancer *in vitro* and *in vivo*, assisting epithelial-mesenchymal transition (EMT) (Xie et al., 2019). In ICD, tyrosine phosphorylation within the half immunoreceptor tyrosine-based activation motif (hem-ITAM) leads to EMT and progression of triple-negative breast cancer (TNBC) (Okita et al., 2017), while serine phosphorylation in position S530 drives TNBC progression *in vitro* and *in vivo* (Wang et al., 2021).

Generally, in normal physiological conditions GPNMB/OA is involved in chondrogenesis and osteogenesis, facilitating tissue repair through regulation of osteoblasts differentiation (Abdelmagid et al., 2007, 2010). Also, OA supports bone resorption through upregulation in osteoclasts (Sheng et al., 2008). Dendritic cell-associated HSPG-dependent integrin ligand (DC-HIL), another name for GPNMB, facilitates transendothelial migration of antigen presenting cells (APC) through binding with its RGD to heparan sulfate proteoglycans on endothelial cells (Shikano et al., 2001). DC-HIL and syndecan-4 axis inhibits the activation of $CD4^+$ and $CD8^+$ T cells (Chung et al., 2009). GPNMB is also expressed in melanocytes, where it regulates the melanosomes synthesis (Zhang et al., 2012).

With the several examples in pathology, GPNMB is not only involved in carcinogenesis from versatile origins, but also induces insulin resistance with further lipogenesis in white adipose tissue, while being secreted by liver (Gong et al., 2019). GPNMB inhibits the terminal differentiation of GLI1 neural stem cells into oligodendrocytes by upregulation of TGFβR2, favoring demyelination of the brain tissue (Radecki et al., 2021). In Alzheimer Disease, GPNMB was reported to correlate with a subset of a distinct microglia population, that cluster around amyloid plaques in patients with profound neural loss, however it is not clear whether glycoprotein plays a protective or a deleterious role (Hüttenrauch et al., 2018).

As previously mentioned, GPNMB profoundly regulates the progression of breast cancer, with TNBC in particular. As a partially discovered mechanism, GPNMB could upregulate PI3K/AKT/mTOR signaling axis and elevate β-catenin activity, which drove breast cancer progression through enhanced canonical Wnt-1 pathway (Maric et al., 2019). On the other hand, in drug-resistant melanoma cases GPNMB and other genes like TRP1, TYR, and PMEL17 were upregulated by microphthalmia-associated transcription factor (MITF) (Rose et al., 2016); the

progression and metastatic behavior of melanoma was dependent on GPNMB immunosuppressive function (Tomihari et al., 2010). In glioblastoma, GPNMB could regulate the tumorigenesis directly through binding with α subunits of Na/K-ATPase, activating PI3K/AKT axis (Ono et al., 2016), as well as, similarly to melanoma case, could regulate through facilitation of immunosuppressive microenvironment (Hudson et al., 2018).

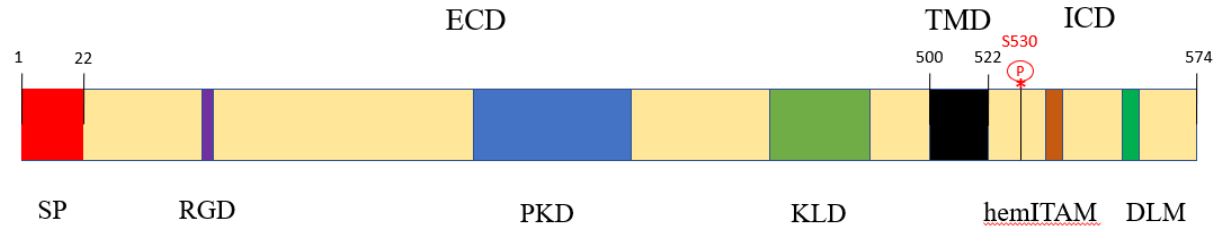

Figure 1.2.1. Schematic structure of GPNMB

ECD – extracellular domain, including SP – signal peptide, RGD – integrin recognition domain, PKD – polycystic kidney disease homology domain, KLD – kringle like domain. TMD – transmembrane domain. ICD – intracellular domain, including S530 – serine phosphorylation site, hem-ITAM - half immunoreceptor tyrosine-based activation motif, DLM – dileucine motif.

1.2.2. GPNMB in HNSCC

Up until recently, there are several reports showing the correlation and function of GPNMB in HNSCC. Arosarena et al. reported that osteoactivin promotes migration of oral SCC (Arosarena et al., 2016). Briefly, they showed OA was highly expressed in various HNSCC cell lines, while the function of OA was controversial. Treatment with recombinant OA (rhOA) could promote cell survival in SCC15 but reduced for UMSCC14a in serum-free-medium condition. Besides, not all tested cell lines were dependent on OA during migration in wound-healing assay. They could co-

precipitate OA and several integrins from α and β subunits, which could activate MAPK signaling indicating and promote cellular migration (Hood & Cheresh, 2002; Rizqiawan et al., 2013). Similar work indicated, that osteoactivin mediates spheroid invasion of HNSCC cell lines (Arosarena et al., 2018). Among different cell lines OA could regulate matrix metalloproteinases (MMPs), increasing MMP-2, -3, -9, -10, depending on the cell line. Two independent reports found high levels of GPNMB expression in tumorous lesions of HNSCC patients (Li et al., 2019; van Schaik et al., 2020). Furthermore, Hanemaaijer et al. reported, that 92% out of 414 samples with HNSCC were GPNMB positive, while their prediction model of best targets for antibody-drug conjugates treatment were GPNMB, SLIT and NTRK family member 6, EGFR, CD74, CD44 (Hanemaaijer et al., 2018). However until now, there is no structured *in vitro* and *in vivo* studies of GPNMB involvement in LSCC carcinogenesis. There is also lack of understanding how GPNMB affects and regulates expression of oncogenes, related to LSCC progression.

1.3. Cancer Stemness

The theory of cancer stem cells (CSCs) occurred last century from leukemia studies (Bonnet & Dick, 1997; Uckun et al., 1995) and recently it attracts more attention. The main principle of this theory is that the viability of the cancer cells and cancer tissue in general is supported by a small population of quiescent in nature cells with self-renewal ability. This justifies the facts of drug resistance, while the targets for chemotherapy are fast proliferative cells. After the treatment, dormant progenitor cells originate new clusters of mutated proliferating cells, maintaining the advancement of cancer (Moore & Lyle, 2011). First studies to reveal CSCs were based on the following method. Initially, from the heterogeneous cancer tissue cells are sorted and isolated. Those isolated cells had a unique feature of surface protein expression; hence some markers were

identified, which indicate populations of CSCs in multiple-origin cancers (Walcher et al., 2020). Cancer stem isolated cells could initiate new populations of cancer cells, while making undifferentiated clones in xenografted immunosuppressed models (O'Brien et al., 2007). Experiments *in vivo* became a general tool to examine phenotypically new CSCs expressing stemness-related biomarkers (Clarke et al., 2006; Wang et al., 2015). Cells are separated based on their surface expression pattern and further transplanted into immunodeficient mice. After the tumor formation cells will be sorted and these steps will be repeated several times. The cells, which can serially induce the tumor formation will be defined as CSCs.

After the leukemia there were reports on the existence of CSCs in breast cancer (Al-Hajj et al., 2003), brain cancer (Singh et al., 2004), and colon cancer (Ricci-Vitiani et al., 2007), while the studies in SCC were not an exclusion (Oshimori et al., 2015). It was reported that CSCs in HNSCC are located on the edges of the invasive cancerous tissues, close to perivascular niches, where signals from endothelium upregulate maintenance and self-renewal ability of CSCs (Krishnamurthy & Nör, 2012). Numerous markers were found to represent different pools of CSCs in HNSCC (Major et al., 2013), which indirectly indicates on heterogeneity of SCC and complexity of treatment discovery. Thus, it is important to reveal upstream molecules which regulate the populations of CSCs within cancers of multiple origins, including LSCC.

CHAPTER 2. MATERIALS AND METHODS

2.1. Cells and cell cultivation

We received HPV negative laryngeal SCC cell lines UMSCC-10A, UMSCC-10B, UMSCC-11A, UMSCC-11B, UMSCC-12, UMSCC-13, and UMSCC-25 from the Head and Neck Cancer Biology Laboratory at the University of Michigan (Ann Arbor, MI, USA). From the American Type Culture Collection (ATCC) we received human embryonic kidney (HEK) 293T cells. The detailed information on cell lines is presented in Table 2.1. For cultivation in 2D monolayer condition, cells were maintained in Dulbecco's Modified Eagle's Medium (DMEM) (Invitrogen), with addition of 10% fetal bovine serum (FBS) (Gibco), 100 µM MEM Non-essential Amino Acids Solution (Wako), 100 U/mL penicillin G (Wako), and 100 µg/mL streptomycin sulfate (Wako). For cultivation in 3D sphere anchorage-independent condition, cells were maintained in serum-free DMEM/F-12 (1:1) medium (Invitrogen), 2% B-27 supplement (Invitrogen), 20 ng/mL bFGF (Sigma), 20 ng/mL EGF (Wako), 100 U/mL penicillin G (Wako), and 100 µg/mL streptomycin sulfate (Wako). To achieve anchor-independent cellular proliferation, 6-well ultra-low-attachment culture dishes (Corning) were utilized. All cell cultures were sustained in incubators with a 5% CO_2-humidified atmosphere at 37°C.

Table 2.1. LSCC cell lines (Brenner et al., 2010)

Cell line	Origin	Specimen site	Grade	TNM	Stage	Previous treatment
UMSCC-10A	true vocal cord	true vocal cord	M-WD	T3N0M0	III	none
UMSCC-10B	larynx	submental lymph node	M-WD	T3N1M0	III	surgery
UMSCC-11A	epiglottis, ipsilateral lymph node	hypopharynx	-	T2N2aM0	IV	pretreatment biopsy
UMSCC-11B	supraglottis, ipsilateral lymph node	hypopharynx	-	T2N2aM0	IV	CT, surgery
UMSCC-12	larynx	larynx	MWD	T2N1M0	III	surgery
UMSCC-13	larynx	esophagus	WD	T3N0M0	III	RT, surgery
UMSCC-25	larynx	neck	PD	T3N0M0	III	RT, surgery

PD – poorly differentiated, MWD – moderately well differentiated, M-WD – moderately to well differentiated, WD – well differentiated. CT – chemotherapy, RT – radiotherapy.

2.2. Construction of DNA-plasmids for short hairpin-mediated knockdown

For experiments with stable knockdown (KD), four short hairpin RNAs (shRNAs) against GPNMB (№1, №2, №3 and №4) (Table 2.2) were designed and obtained according to Addgene protocol for pLKO.1 – TRC Cloning Vector construction. Oligonucleotides were annealed in 10% NEB2 M (Takara) buffer, then ligated with a pre-digested (EcoR1 and Age1 restriction sites) pLKO.1-puro (Addgene #10878) vector at 16°C overnight. The shRNA with a non-targeting sequence in the pLKO.1-puro vector was used as a control (shRNA#con) (Table 2.2). After the transfer of ligated plasmids into E. coli (DH5α), initiation and propagation of bacterial colonies was dependent on successful ligation of pLKO.1-puro plasmids with resistance to ampicillin, later colonies were further cultured in LB medium with ampicillin at 37°C. Next, amplified colonies were subjected to extraction of DNA using FastGene® Plasmid Mini Kit according to the standard protocol. Later, fragments of amplified plasmids were checked by cutting at EcoR1 and at Nco1 restriction sites, the sequences of shRNA-plasmids were examined, and successful clones were chosen for the final DNA extraction. All four successfully constructed plasmids were transfected into HEK 293T cells with overexpressed (OE) GPNMB, and their efficiency was examined by protein quantification, using Western blotting method. From oligosequences, presented in Table 2.2, numbers 1 and 4 were chosen for subsequent experiments and were named shRNA#1 and shRNA#2 respectively. The virus was constructed using packaging psPAX2 (Addgene #12260), envelope pMD2.G (Addgene #12259), and pLKO.1-shRNA plasmids. All plasmids were transfected using PEI transfection reagent (Polysciences Asia-Pacific) into HEK 293T cells. Media were changed, collected with constructed virus, and filtered through 0.22 μm membrane. Viral solutions were aliquoted and kept in -80°C.

Table 2.2. Sequences of oligonucleotides

Name	Forward (5'-3')	Manufacturer
shRNA#con	GCGCGCTTTGTAGGATTCG	OligoEngine
shRNA#1 (№1)	AACATTTGCGGTGAACCTGAT	Invitrogen
№2	AATTGGGACGATGTTCAGTGA	Invitrogen
№3	AAATTCATCCGACGAAACCTT	Invitrogen
shRNA#2 (№4)	AACTGCCAGATTAACAGATAT	Invitrogen

2.3. Knockdown using lentiviral system

UMSCC-11A and UMSCC-11B cells were seeded for examination of resistance to Puromycin. From the range of 0 µg/ml to 2 µg/ml of Puromycin in 2D culture medium, cells were cultured for 4 days. The least concentration of Puromycin was chosen, which could successfully eliminate culturing cells. That is 1 µg/mL for UMSCC-11A and 0.5 µg/mL for UMSCC-11B. Next, cells were seeded into 6 – well plates (Falcon) and subjected to infection with lentiviral solution, including 8 µg/mL Polybrene (Sigma). Subsequently, the medium was changed to Puromycin-containing medium with desired concentration and selection was performed for 4 days.

2.4. Western blotting

Cells were washed with PBS, trypsinized, and centrifugated at 1000 rpm for 5 minutes. After supernatant was removed, cell pellets were subjected to lysis with Nonidet® P-40 (NP-40, Nacalai Tesque, Inc.) buffer during 20 minutes at 4°C. Consequently, protein concentration was quantified using a DC Protein Assay (Bio-Rad) according to the manufacturer's protocol, and concentrations were equalized among samples. Next, lysates were solubilized in Sodium Dodecyl Sulfate–

Polyacrylamide (SDS) buffer. Consequently, after the temporal boiling at 98°C, the total cell lysates were subjected to 10% SDS–polyacrylamide gel electrophoresis (SDS-PAGE) and blotted towards a polyvinylidene difluoride (PVDF) membrane (Merck Millipore). For blocking step, the membrane was incubated in 5% skim milk resolved in Tris-buffered saline with Tween® 20 (TBST) buffer for 1 hour in room temperature. The blocked PVDF membrane was further incubated with primary antibodies overnight at 4°C. The detailed list of antibodies is presented in a Table 2.4. After the incubation step, PVDF membrane was washed 3 times for 10 minutes in TBST buffer. Following the washing step, immunoblotted membrane was incubated with secondary antibodies conjugated with horseradish peroxidase (HRP) (Table 2.4) for 30 minutes in room temperature. Subsequently, membrane was washed in TBST buffer 3 times for 10 minutes, and proteins were detected by applying chemiluminescent kit ImmunoStar® Zeta, according to the manufacturer's instructions, using EZ capture MG imaging system (ATTO Corporation, Tokyo, Japan).

Nonidet® P-40 (NP-40) buffer	1% NP-40, 2% 1M Tris-HCl (pH 7.5), 3% 5M NaCl, 0.2% Aprotinin (Invitrogen), and 0.2% Leupeptin (Invitrogen)
Sodium Dodecyl Sulfate–Polyacrylamide (SDS) buffer	2% SDS, 5% 2-mercaptoethanol (Wako), 10% glycerol, 62.5 mM Tris-HCl (pH 7.5), 2% dithiothreitol (DTT), and 0.002% bromophenol blue
SDS–polyacrylamide gel electrophoresis (SDS-PAGE), 10%, 16x16 cm	1) Running gel: MQ 7.6 ml, 30% Acrylamide (Wako) 5.2 ml, 2 M Tris-HCl (pH 8.8) 3.2 ml,

	10% SDS 80 µl, 10% APS 72 µl, N-N-N-N-tetramethyl-ethylenediamine (Wako) 16 µl 2) Stacking gel: 20% Glycerol 3.5 ml 30% Acrylamide (Wako) 700 µl, 0.5 M Tris-HCl (pH 6.8) 700 µl, 10% SDS 25 µl, 10% APS 25 µl, N-N-N-N-tetramethyl-ethylenediamine (Wako) 5 µl
Tris-buffered saline with Tween® 20 (TBST) buffer	10 mM Tris-HCl (pH 7.4), 150 mM NaCl, 0.1% Tween® 20

Table 2.4. Antibodies

Primary antibodies

Target	**Catalog**	**Manufacturer**	**Dilution (IHC)**	**Dilution (IF)**	**Dilution (WB)**
GPNMB	AF2550	R&D Systems	1:200	1:200	1:2000
Ki-67	ab15589	Abcam	1:500	1:250	-
GAPDH	sc-32233	Santa Cruz	-	-	1:1000

Secondary Antibodies

Target	Catalog	Manufacturer	Dilution (IF)	Dilution (WB)
Alexa 488 anti-goat IgG	A11055	Invitrogen	1:200	-
Alexa 546 anti-rabbit IgG	A10040	Life Technologies	1:200	-
HRP anti-goat IgG	P0160	Dako	-	1:10000
HRP anti-mouse IgG	NA931V	GE Healthcare	-	1:10000

2.5. Reverse transcription and quantitative PCR analysis

Cells were lysed by TRIzol (Life Technologies) for total RNA isolation. RNA was extracted according to manufacturer's protocol. Reverse transcription was performed with High-Capacity RNA-to-cDNA Master Mix (Applied Biosystems) following the manufacturer's method. Quantitative PCR (qPCR) analysis was done with SYBR Green I qPCR Master Mix (Applied Biosystems) and data were measured by QuantStudio 5 (Thermo Fisher Scientific). Expression levels of the targets were normalized to *β-actin* levels. Experiments were triplicated and data represented as the mean of triplicate wells. Primer sequences are listed in Table 2.5.

Table 2.5. Primers for qRT-PCR

Target	Forward (5'-3')	Reverse (5'-3')
β-actin	GCACTCTTCCAGCCTTCCTT	CGTACAGGTCTTTGCGGATG
GPNMB	TCACCCAGAACACAGTCTGC	CAGACCCATTGAAGGTTCGT
BMI1	GAGGGTACTTCATTGATGCCACCAAC	GCTGGTCTCCAGGTAACGAACAATA
SOX2	TGCGAGCGCTGCACAT	TCATGAGCGTCTTGGTTTTCC
NANOG	TTCCTTCCTCCATGGATCTG	CTTTGGGACTGGTGGAAGAA
MSI1	GGGACTCAGTTGGCAGACTAC	CTGGTCCATGAAAGTGACGAA
KLF4	CCTTCCTGCCCGATCAGATG	GGTGAAGAAGGTGGGGTGAG
PROM1	TTGCGGTAAAACTGGCTAAG	TGGGCTTGTCATAACAGGAT
ALDH1A1	TGTTAGCTGATGCCGACTTG	CTGGCCCTGGTGGTAGAATA
CD44	GGCTTTCAATAGCACCTTGC	CAGGTCTCAAATCCGATGCT
POU5F1	AGTGAGAGGCAACCTGGAGA	ACACTCGGACCACATCCTTC
DEFB4A	CTCCTCTTCTCGTTCCTCTTCA	GCAGGTAACAGGATCGCCTAT

2.6. Proliferation assay in 2D

Four thousand cells per well were seeded in triplicate in 96-well flat-bottom polystyrene plates (TPP®). Cellular proliferation was measured by a CellTiter 96®AQueous One Solution Cell Proliferation Assay (MTS assay; Promega) according to the manufacturer's protocol. The optical density of coated microplates was measured by Varioskan LUX Multimode Microplate Reader (Thermo Fisher Scientific). Experiments were repeated three times and are presented as the mean of triplicate wells.

2.7. Tumor sphere formation assay

Ten thousand cells per well were seeded in triplicate in ultra-low attachment 6-well plates (Corning) and cultivated in culture medium for 3D sphere condition. In GPNMB stable KD cell lines the sizes and numbers of spheres with diameters of more than 150 μm were counted on day 7. To determine the expression of CSCs genes in stable GPNMB KD cell lines, 10^5 cells per well were seeded in ultra-low attachment 6-well plates and cultured for 3 days. Spheres were collected by centrifugation and subjected to the next step of mRNA isolation. In DEFB4A KD experiments the numbers and sizes of spheres with diameters of more than 100 μm for UMSCC-11A and more than 60 μm for UMSCC-11B were counted on day 3.

2.8. Wound-healing scratch assay

Cells were seeded for confluency in triplicate to 12-well plates (Falcon) and maintained in 2D monolayer culture medium. Following 12 h of adhesion, a cross-shape scratch was applied into the culture. Pictures of scratched wounds were taken twice and relative ratio of healing/closure was quantified by pixel percentages with ImageJ software (National Institutes of Health). The time of migration for UMSCC-11A was 16 hours after application of a scratch and 23 hours for UMSCC-11B.

2.9. Analysis of mRNA sequencing

After the isolation and extraction of total mRNA by TRIzol (Life Technologies), pellets containing mRNAs were dissolved in 30 μL of MQ, and integrity of mRNAs was checked by implementing Agilent RNA 600 Nano Kit (Cat# 5067-1511; Agilent) by a Bioanalyzer (Agilent). While the RNA Integrity Number (RIN) within all samples was 10, those RNAs were subjected to library

preparations for mRNA-sequencing. The libraries were created by applying 2.5 µg of each sample's RNA using NEBNext Ultra II RNA Library Prep Kit for Illumina and NEBNext Poly(A) mRNA Magnetic Isolation Module (New England Biolabs, Cat# E7770S and E7490L) according to the manufacturer's instructions. Concentrations and size distributions of the libraries were measured using Agilent DNA 7500 kit (Cat#5067-1506; Agilent) by the Bioanalyzer. Following the creation, libraries were diluted to 1 nM and subjected to denaturation and neutralization. Afterwards, libraries were adjusted to 1.8 pM and sequenced by NextSeq 500 System (Illumina) using NextSeq500/550 v2.5 (75 Cycles) Kits (Illumina, Cat#20024906). The sequencing was performed with paired-end reads of 36 bases. After the run, FASTQ files were extracted, and information of the next-generation sequencing run data was checked on CLC Genomics Workbench 20.0.3 software (CLC, QIAGEN) to identify GPNMB-KD mediated changes in the mRNA expression profile. Finally, the PHRED-score (quality score of the reads) over 20 was confirmed for 99% of the reads, indicating a successful run.

2.10. Analysis of RNA-sequencing results

Differentially expressed genes (DEGs) were restricted with false discovery rates (FDR *p*-value) set at < 0.05 and a 1.5-fold-change cutoff. Obtained DEGs were categorized into cellular migration, cellular proliferation (according to the GSEA database) (GO:0016477; GO:0050673), and lymphovascular-invasion-related genes (Zhang et al., 2020). Heatmaps were constructed in Prism GraphPad version 8 software using standardized Transcripts Per Kilobase Million (TPM) expression values.

2.11. Formation of tumors *in vivo*

Xenograft experiments were performed with five-week-old female BALB/cAJcl-*nu/nu* mice kept under SPF conditions (CLEA Japan). One million cells from each stable GPNMB KD condition were subcutaneously injected to form 3 experimental groups (shRNA#con, shRNA#1, and shRNA#2). Following subcutaneous introduction, mice were sacrificed at 10 (for UMSCC-11A) and 6 (for UMSCC-11B) weeks. Next formula was used to calculate volumes of the extracted xenografts: $V(\text{volume}) = \pi L(\text{length})W^2(\text{width})/6$. The conduction of animal experiments was approved by the Animal Ethics Committee of the University of Tsukuba in accordance with the University's animal experiment guidelines and the provisions of the 1995 Declaration of Helsinki.

2.12. LSCC patients and tissue specimens

Seventy-six formalin-fixed, paraffin-embedded (FFPE) clinical tissue samples were obtained from 59 LSCC patients with a single or several surgeries in medical history (Table 2.12). To perform experiments in this study, patients' consents and the approval from the Ethical Review Committee of University of Tsukuba Hospital were acquired. The number of the project is R02-147.

Table 2.12. Clinical specimens from LSCC patients

Number of specimens	Manipulation
36	Total laryngectomy
33	Laryngeal microsurgery
4	Neck dissection
2	Transoral CO2 laser & laryngoscopy surgeries
1	Partial laryngotomy

2.13. Immunohistochemical and immunofluorescence staining

Formalin fixed, paraffin-embedded (FFPE) specimen sections were deparaffinized in xylene, with further rehydration in ethanol, and autoclaved for 20 minutes in NaOH-citrate buffer at 121°C to retrieve antigenicity. Blocking solution (Perkin Elmer Life Science) was used to suppress nonspecific antibody reactions, then sections were incubated with primary antibodies, dilutions are indicated in Table 2.4. For immunohistochemical (IHC) staining, reacted antibodies were detected by the Dako EnVision + System/HRP (DAB, DakoCytomation). To perform quantification analysis, I used NanoZoomer Digital Pathology system (2.0RS, Hamamatsu) and the QuPath software (Bankhead et al., 2017). For immunofluorescent (IF) staining, sections were incubated with secondary fluorescent-labeled antibodies and then mounted with DAPI Fluoromount-G® (SouthernBiotech) for nuclei staining. The fluorescence microscope (Keyence BZ-X710) was utilized for detection and imaging.

2.14. ELISA sandwich assay

These experiments were performed to quantify the sGPNMB concentration within serum samples of LSCC patients and of non-malignant group. The enzyme-linked immunoassay was performed using DuoSet® ELISA Human Osteoactivin/GPNMB kit (Catalog #DY2550, R&D Systems) and DuoSet® Ancillary Reagent Kit2 (Catalog #DY008, R&D Systems) according to manufacturer's instructions. Twenty-two samples of LSCC cases and thirty samples of control cases were diluted 10 times by Reagent Diluent x1. The optical density of coated microplates was measured by Varioskan LUX Multimode Microplate Reader (Thermo Fisher Scientific). Photometric results were obtained by 450 nm and 570 nm wavelengths reads with further wavelength correction. The standard curve was created by Rodbard equation in Image J software (National Institutes of Health).

Parameters were extracted and used to quantify the concentration of each 10 times diluted sample (x) from the next formula: y = d+(a-d)/(1+(x/c)^b). Results were multiplied 10 times to receive the concentration of undiluted samples. Results are presented as the mean of triplicate wells.

2.15. Statistical analysis

Quantitative data are represented as the means ± standard deviations (SDs). Statistical analyses were performed using one-way or two-way analyses of variance (ANOVA) with the Tukey's multiple comparison test using GraphPad Prism 8 software. Probability values (*p* value) less than 0.05 were considered statistically significant.

CHAPTER 3. RESULTS

3.1. GPNMB is highly expressed in HNSCC and LSCC

Firstly, I analyzed the GPNMB mRNA expression levels in HNSCC samples in comparison with non-malignant samples using The Cancer Genome Atlas (TCGA) publicly available database by UALCAN web resource (Chandrashekar et al., 2017). In carcinoma tissues, mRNA levels of GPNMB were significantly increased in all clinical stages and grades compared with non-malignant tissues (Fig. 3.1 A, B, C; Table 3.1). However, according to data obtained from the Kaplan-Meier Plotter database (Nagy et al., 2021) of patients with HNSCC, the expression of GPNMB was not significantly different between the poor and the positive prognostic groups in the OS analysis (Fig. 3.1 D). To evaluate the role of GPNMB in LSCC, I analyzed GPNMB protein and mRNA expression levels in seven laryngeal SCC cell lines: UMSCC-10A, -10B, -11A, -11B, -12, -13, and -25 (Fig. 3.1 E, F; Table 2.1). All LSCC cell lines, excluding UMSCC-12, exhibited diversified expression patterns of GPNMB protein and mRNA levels. At the same time, GPNMB mRNA and protein levels were identical in each UMSCC laryngeal cell line. The results of these experiments denote enhanced expression of GPNMB in HNSCC patient tissues and in LSCC cell lines.

3.2. GPNMB silencing impairs cellular proliferation, sphere formation, and cellular migration of LSCC cell lines

To examine the role of GPNMB in carcinogenesis, I established stable KD cells from UMSCC-11A and -11B by infection with a constructed lentivirus expression system using two independent

shRNAs against GPNMB (shRNA#1 and shRNA#2) and one shRNA with a non-targeting sequence (shRNA#con). I used WB and qRT-PCR analyses to confirm the efficiency of GPNMB KD. Expectedly, expression levels of GPNMB were significantly decreased (Fig. 3.2 A-F). Afterwards, I defined the proliferative ability of UMSCC-11A and -11B in monolayer 2D condition by an MTS assay, discovering that in both cell lines the growth rate of GPNMB-KD cells was significantly decreased compared to the control (Fig. 3.2 G, H). To determine the role of glycoprotein NMB in anchorage-independent 3D proliferation, I assessed the sphere formation ability of UMSCC-11A and -11B cell lines. Results showed GPNMB-KD cells had impaired 3D growth with significantly fewer spheres (diameter ≥ 150 μm) compared to controls in both cell lines (Fig. 3.2 I-N). Next, I examined the role of GPNMB in cellular migration by performing wound-healing scratch assays (Fig. 3.2 O-R). Similar to previously reported results using oral SCC cells (Arosarena et al., 2016), the GPNMB silencing effect in UMSCC-11A, -11B laryngeal cell lines significantly hindered migration ability compared to the control. These results confirm the function of GPNMB as a key mediator of LSCC monolayer 2D proliferation, of anchorage-independent 3D sphere growth, and of cellular migration.

3.3. GPNMB silencing downregulates cellular proliferation, migration, and lymphovascular-invasion-related genes

Thereafter, I investigated the effect of GPNMB silencing in UMSCC-11A and -11B cells on other genes by RNA-sequence analysis. After the introduction of cutoff criteria on the genes expression data (false discovery rates (FDR) < 0.05 and greater than 1.5-fold-change), I assessed commonly affected genes (DEGs) in stable GPNMB KD cell lines. I found that the majority of cellular migration and cellular proliferation genes were downregulated compared to control in both cell

lines, which was consistent with *in vitro* results (Fig. 3.3 A-D). Interestingly, lymphovascular-invasion-related (LVI) genes (Zhang et al., 2020) (*TTK*, *DEPDC1*, *KIF23*, *KIF18B*, *CCNA2*, and *PRC1*) were also downregulated in the case of UMSCC-11B GPNMB KD cells (Fig. 3.3 E). The summary of pathways enriched via GPNMB silencing is presented in Figure 3.3 F. I have also illustrated top 30 most significantly upregulated and downregulated genes, which carry versatile oncogenic roles (Table 3.3). These data suggest that GPNMB regulates the expression of various cellular proliferation and cellular migration genes in both cell-lines, and furthermore, affecting the expression of LVI -related genes in UMSCC-11B.

3.4. GPNMB silencing impairs tumor formation of LSCC cell lines *in vivo*

As far as GPNMB silencing affects numerous oncogenes *in vitro*, I further studied GPNMB *in vivo* role in carcinogenesis of laryngeal SCC by subcutaneous inoculation of stable GPNMB KD UMSCC-11A and -11B cells into nude mice. GPNMB silencing reduced tumor growth and resulted in significantly decreased tumor volume and weight (Fig. 3.4 A-F). Extracted tumors were subsequently subjected to IHC staining, the analysis revealed that GPNMB protein expression levels were diminished in GPNMB-KD tumors compared to control, while the ratio of Ki-67-positive cells was not significantly different between GPNMB-KD and control tumors (Fig. 3.4 G, H). Additionally, IHC data showed the tendency of cells to differentially express GPNMB and Ki-67 (Fig. 3.4 G, H). To further understand this phenomenon, I performed IF staining of shRNA#con tumors (Fig. 3.4 I, J). The findings from this experiment uncovered a mutually inverse relationship between GPNMB and Ki-67 expressions, in which the majority of GPNMB-positive cells did not express Ki-67 and vice versa. These results show the key role of GPNMB in the tumorigenic

growth of laryngeal SCC cells *in vivo*, as well as the inverse relationship between GPNMB and Ki-67 proteins suggests that GPNMB expression correlates with quiescent, non-proliferating cells.

3.5. The effect of GPNMB KD on CSCs markers in LSCC cell lines

As the previous findings suggested the correlation of GPNMB and non-proliferating cells, I further elucidated the involvement of GPNMB silencing in regulation of cancer stem cell markers expression in UMSCC-11A and -11B. Such CSCs markers as *BMI1*, *ALDH1A1*, *KLF4*, *PROM1* (CD133), *SOX2*, *NANOG*, *POU5F1* (OCT4), *CD44*, and *MSI1* are reported to correlate with CSCs population in HNSCC (Lee et al., 2017; Lee et al., 2014; Major et al., 2013; Xiao et al., 2018; Yu et al., 2013). After obtaining cDNA from GPNMB KD cell lines I quantified the relative expression of abovementioned markers (Fig. 3.5 A, B). Results showed that GPNMB KD significantly decreased the mRNA expression of *BMI1* in both cell lines. However, other genes showed inconclusive data between shRNA#1 and #2 GPNMB KD, as differences in expressions between UMSCC-11A and -11B. These results suggest that GPNMB is involved in *BMI1* regulation, though how GPNMB affects other CSCs-related genes remains controversial.

3.6. GPNMB is expressed in malignant lesions of LSCC patients

To investigate the patterns of GPNMB expression in laryngeal SCC tumors, I obtained and analyzed 76 tissue specimens from 59 LSCC patients (Table 2.12). I compared the expression of GPNMB between cancerous lesions and normal squamous epithelium (if available in the specimen). The representative case shown in Figures 3.6 A-C indicated overexpression of GPNMB in malignant lesions while the expression in normal epithelial layers was undetectable. Interestingly, the data from QuPath (Bankhead et al., 2017) analysis based on IHC staining did not

show significant correlation between GPNMB expression and clinical advancement of LSCC (Fig. 3.6 E-I). To confirm the results from two *in vivo* models of mutually exclusive expression between GPNMB- and Ki-67-positive cells, I conducted IF analysis of a representative sample (Fig. 3.6 D). Similar to Figures 3.4 I-J, most GPNMB-negative cells were Ki-67-positive and in contrary. These findings verify that expression of GPNMB in laryngeal SCC lesions is higher than in normal squamous epithelium and, together with that, the inverse correlation in expression patterns between GPNMB and Ki-67 proteins in primary human LSCC cells.

3.7. Soluble GPNMB in LSCC patients and non-malignant cohort

As GPNMB was significantly upregulated in HNSCC patients, according to TCGA database (Fig. 3.1 A-C; Table 3.1), and it was overexpressed in tumorous lesions of LSCC patients (Figures 3.6 A-C), I aimed to examine the soluble GPNMB (sGPNMB) concentrations in serum samples of laryngeal SCC patients to assess its capacity as a biomarker. For this experiment I included serum samples from 22 patients diagnosed with SCC in larynx and 30 serum samples from the patients with no malignancy or diabetes mellitus. Next, I measured the sGPNMB levels using kits described in material and methods (Fig. 3.7). However, results did not show a significant difference in expression of sGPNMB between LSCC cases and control. Moreover, isolated cases in both groups were reaching prominent levels of concentration (up to 131,159.2 pg/mL). These outcomes suggest that the cleaved form of GPNMB cannot be used as a biomarker from the systemic blood circulation to suspect such malignancy as LSCC.

3.8. GPNMB knockdown-mediated DEFB4A upregulation leads to suppression of sphere formation in UMSCC-11B

Besides the DEGs related to cellular proliferation, migration, or LVI-mediated processes (Figure 3.3 C-E), one of the most significantly upregulated genes in GPNMB KD cell-lines is *DEFB4A* (Table 3.3). According to the TCGA database, UALCAN web resource analysis (Chandrashekar et al., 2017) showed no significant increase of *DEFB4A* mRNA levels between clinical stages compared to normal tissue (Fig. 3.8 A, B). Interestingly, the expression pattern based on differentiation grades and nodal status of HNSCC cohort showed a significant decrease of *DEFB4A* in lower differentiation grades (Grade 3, 4) and in advanced metastatic cases (N2, N3) (Fig. 3.8 C, D). Subsequently, according to data obtained from the Kaplan-Meier Plotter database (Nagy et al., 2021) of HNSCC patients, *DEFB4A* expression was not significantly upregulated in cases with positive OS (Fig. 3.8 E). After I confirmed expression differences of this gene in GPNMB KD UMSCC-11A and UMSCC-11B by qRT-PCR (Fig. 3.8 F, G), I performed DEFB4A knockdown in shRNA#2 GPNMB KD cells (as most *DEFB4A* upregulated condition) using transfection of DEFB4A siRNA (siRNA#1 and #2) (Fig. 3.8 H, I). Consequently, I assessed the tumorigenic effect of DEFB4A silencing in GPNMB KD cells via sphere formation assay (Fig. 3.8 J-M). Interestingly, silencing of DEFB4A resulted in significant recovery of sphere formation in UMSCC-11B, but not in UMSCC-11A. These findings suggest that GPNMB KD-mediated upregulation of DEFB4A leads to suppression of sphere formation in UMSCC-11B cell-line.

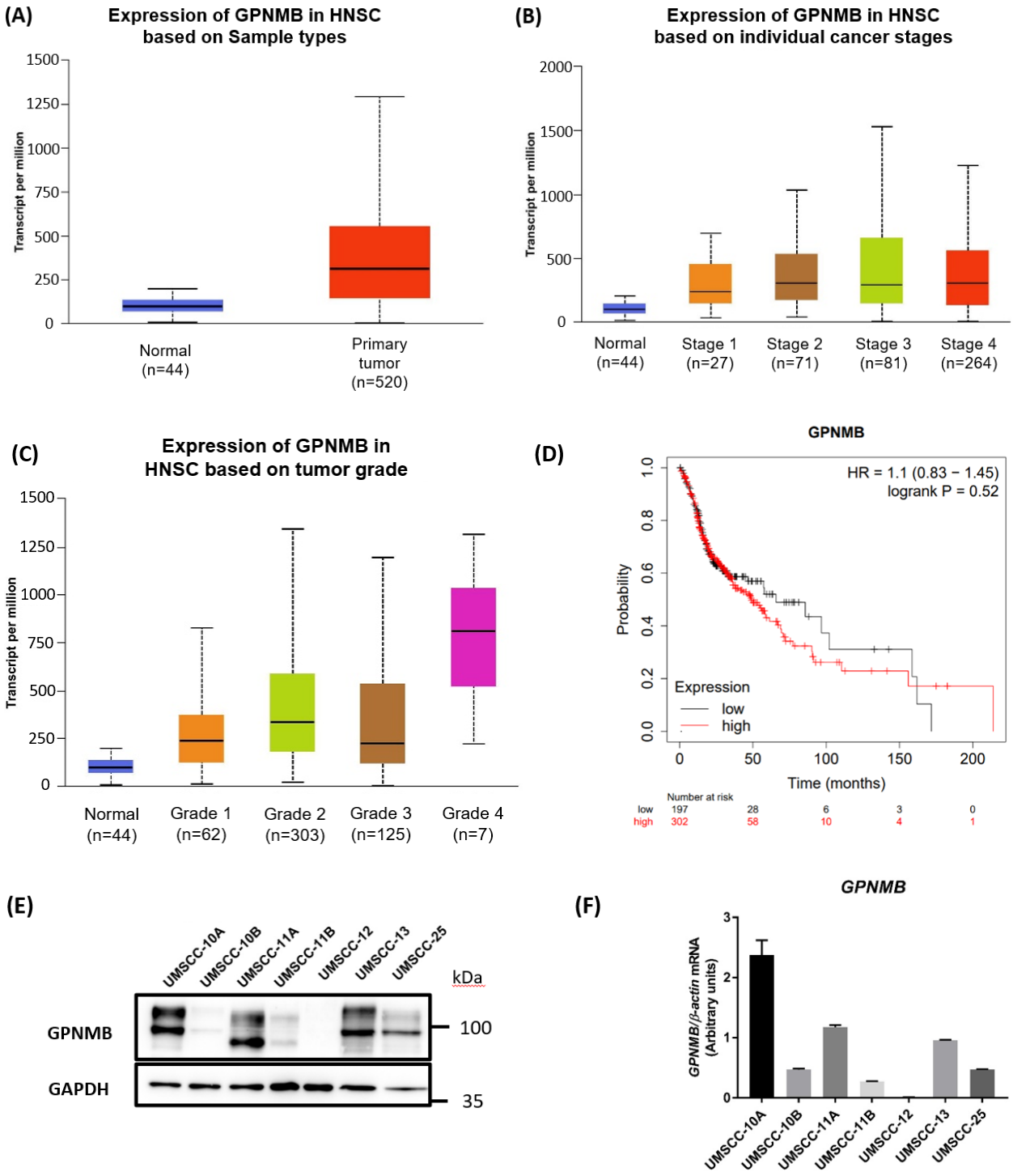

Figure 3.1. Elevated expression of GPNMB in patients with HNSCC and LSCC cell lines

(A) *GPNMB* mRNA profile in primary head and neck squamous cell carcinoma (HNSC) specimens and normal specimens from the TCGA database (UALCAN analysis). **(B, C)** *GPNMB*

mRNA profile in primary HNSC specimens with different clinical stages and tumor grades compared to normal specimens from the TCGA database. Respectively, grades 1 to 4 are defined as: well differentiated, moderately differentiated, poorly differentiated, undifferentiated subtypes. **(D)** Overall Survival (OS) results of *GPNMB*$^{high/low}$ in patients with HNSCC from Kaplan-Meier Plotter analysis. **(E)** Results of western blot analysis exhibiting differentially expressed GPNMB in laryngeal SCC cell lines. GAPDH was utilized as a loading control. Data represents one of three independent experiments. **(F)** mRNA expression levels of *GPNMB* in LSCC cell lines were normalized to *β-actin*. Results are shown as means ± SD, a representative of triplicated experiments.

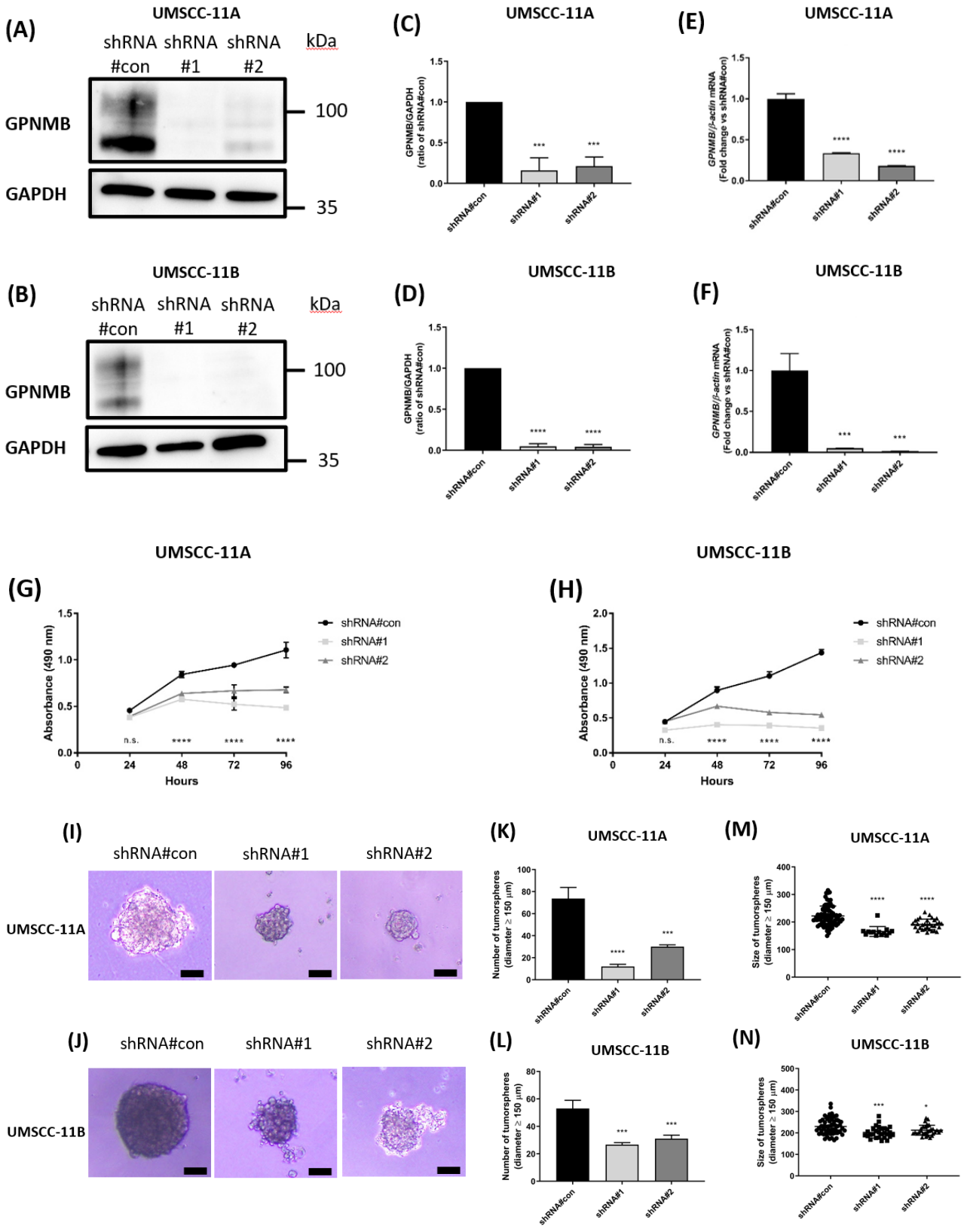
(A)
UMSCC-11A
shRNA #con
shRNA #1
shRNA #2
kDa
GPNMB
GAPDH
100
35
(B)
UMSCC-11B
(C)
UMSCC-11A
GPNMB/GAPDH (ratio of shRNA#con)
shRNA#con
shRNA#1
shRNA#2
(D)
UMSCC-11B
(E)
UMSCC-11A
GPNMB/β-actin mRNA (Fold change vs shRNA#con)
(F)
UMSCC-11B
(G)
UMSCC-11A
Absorbance (490 nm)
Hours
n.s.
(H)
UMSCC-11B
(I)
shRNA#con
shRNA#1
shRNA#2
UMSCC-11A
(J)
UMSCC-11B
(K)
UMSCC-11A
Number of tumorspheres (diameter ≥ 150 μm)
(L)
UMSCC-11B
(M)
UMSCC-11A
Size of tumorspheres (diameter ≥ 150 μm)
(N)
UMSCC-11B

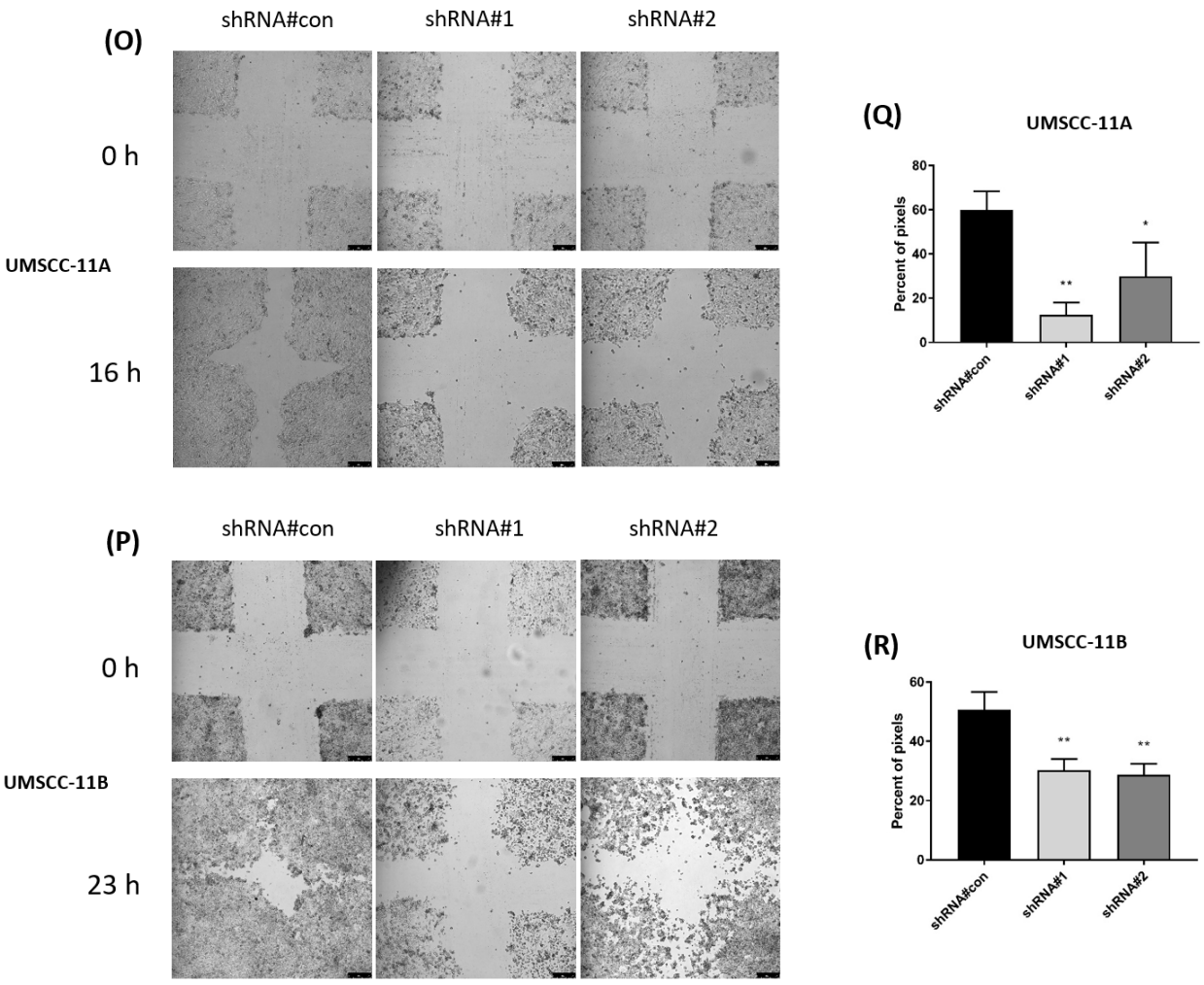

Figure 3.2. Role of GPNMB for laryngeal SCC cell lines in monolayer, anchorage-independent cellular proliferation, and cellular migration *in vitro*

(A - D) Western blot analyses and protein expression quantification data for GPNMB and GAPDH detection in UMSCC-11A and -11B cells of shRNA#control and GPNMB knockdown (KD) (shRNA#1 and shRNA#2). **(E, F)** qRT-PCR analysis of *GPNMB* mRNA in UMSCC-11A, -11B with GPNMB KD. Messenger RNA expression levels were normalized to *β-actin*. **(G, H)** MTS assay results of monolayer cell proliferation in UMSCC-11A, -11B GPNMB KD cell lines. **(I, J)** Representative photos and **(K-N)** results indicate numbers and sizes of 3D spheres formed by

UMSCC-11A, -11B with GPNMB KD. Scale bars are 100 µm. For both cell lines only spheres ≥ 150 µm in diameter were counted. **(O - R)** Wound-healing scratch assay of UMSCC-11A and of UMSCC-11B with GPNMB KD. Photos represent the wound-healing scratch assay. Scale bars are 250 µm. The closed wound fracture area was measured by ImageJ prior to the open area at 0 h. All data are presented as means ± SD, representative of three independent experiments. n.s., not significant, *$p < 0.05$, **$p < 0.01$, ***$p < 0.001$, ****$p < 0.0001$ one-way ANOVA (C-F, I-L, N, P) and two-way ANOVA (E-F) with Tukey's multiple comparison test.

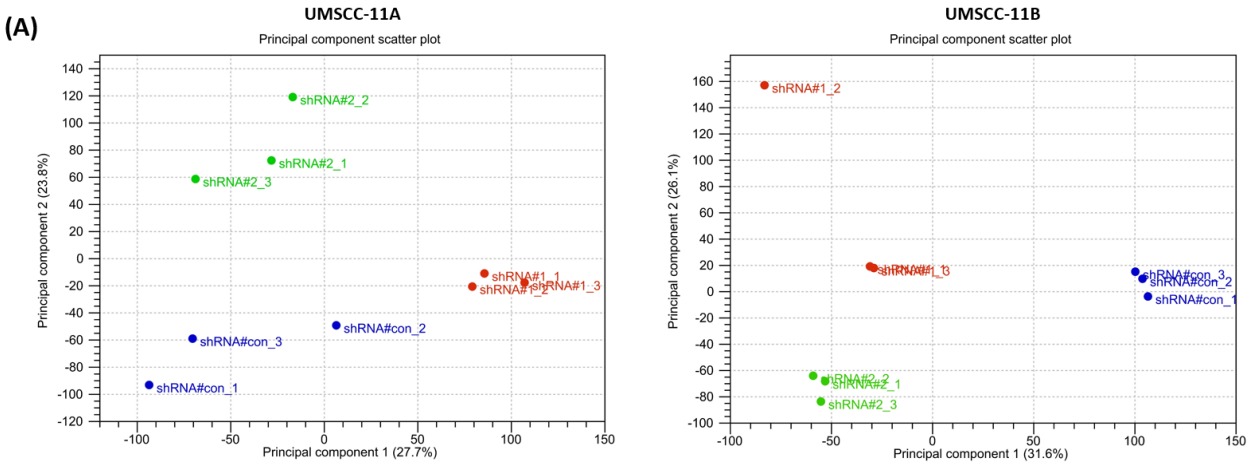
(A)
UMSCC-11A
Principal component scatter plot
Principal component 2 (23.8%)
Principal component 1 (27.7%)
shRNA#2_2
shRNA#2_1
shRNA#2_3
shRNA#1_1
shRNA#1_2
shRNA#1_3
shRNA#con_2
shRNA#con_3
shRNA#con_1
UMSCC-11B
Principal component scatter plot
Principal component 2 (26.1%)
Principal component 1 (31.6%)
shRNA#1_2
shRNA#con_3
shRNA#con_2
shRNA#con_1
shRNA#2_2
shRNA#2_1
shRNA#2_3

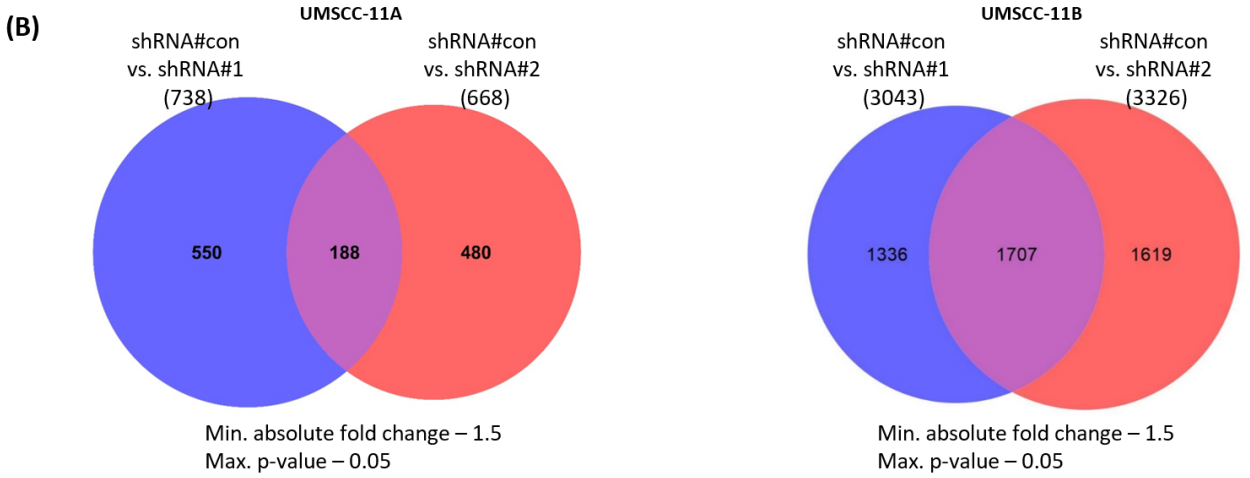
(B)
UMSCC-11A
shRNA#con vs. shRNA#1 (738)
shRNA#con vs. shRNA#2 (668)
550
188
480
Min. absolute fold change – 1.5
Max. p-value – 0.05
UMSCC-11B
shRNA#con vs. shRNA#1 (3043)
shRNA#con vs. shRNA#2 (3326)
1336
1707
1619
Min. absolute fold change – 1.5
Max. p-value – 0.05

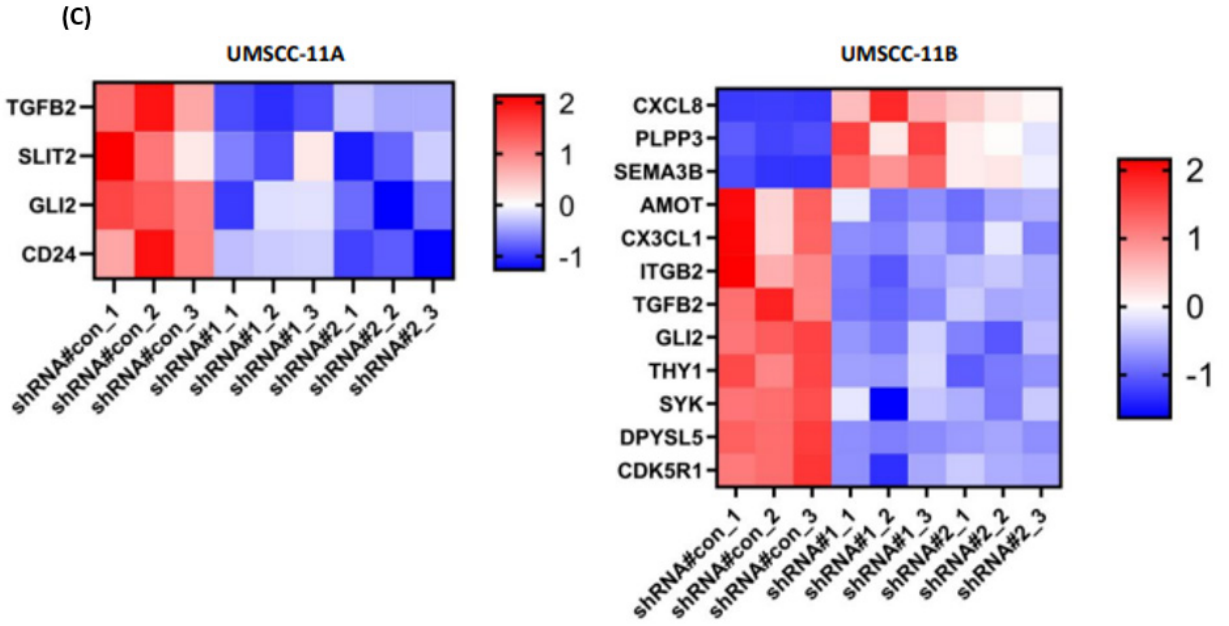
(C)
UMSCC-11A
TGFB2
SLIT2
GLI2
CD24
shRNA#con_1
shRNA#con_2
shRNA#con_3
shRNA#1_1
shRNA#1_2
shRNA#1_3
shRNA#2_1
shRNA#2_2
shRNA#2_3
2
1
0
-1
UMSCC-11B
CXCL8
PLPP3
SEMA3B
AMOT
CX3CL1
ITGB2
TGFB2
GLI2
THY1
SYK
DPYSL5
CDK5R1
shRNA#con_1
shRNA#con_2
shRNA#con_3
shRNA#1_1
shRNA#1_2
shRNA#1_3
shRNA#2_1
shRNA#2_2
shRNA#2_3
2
1
0
-1

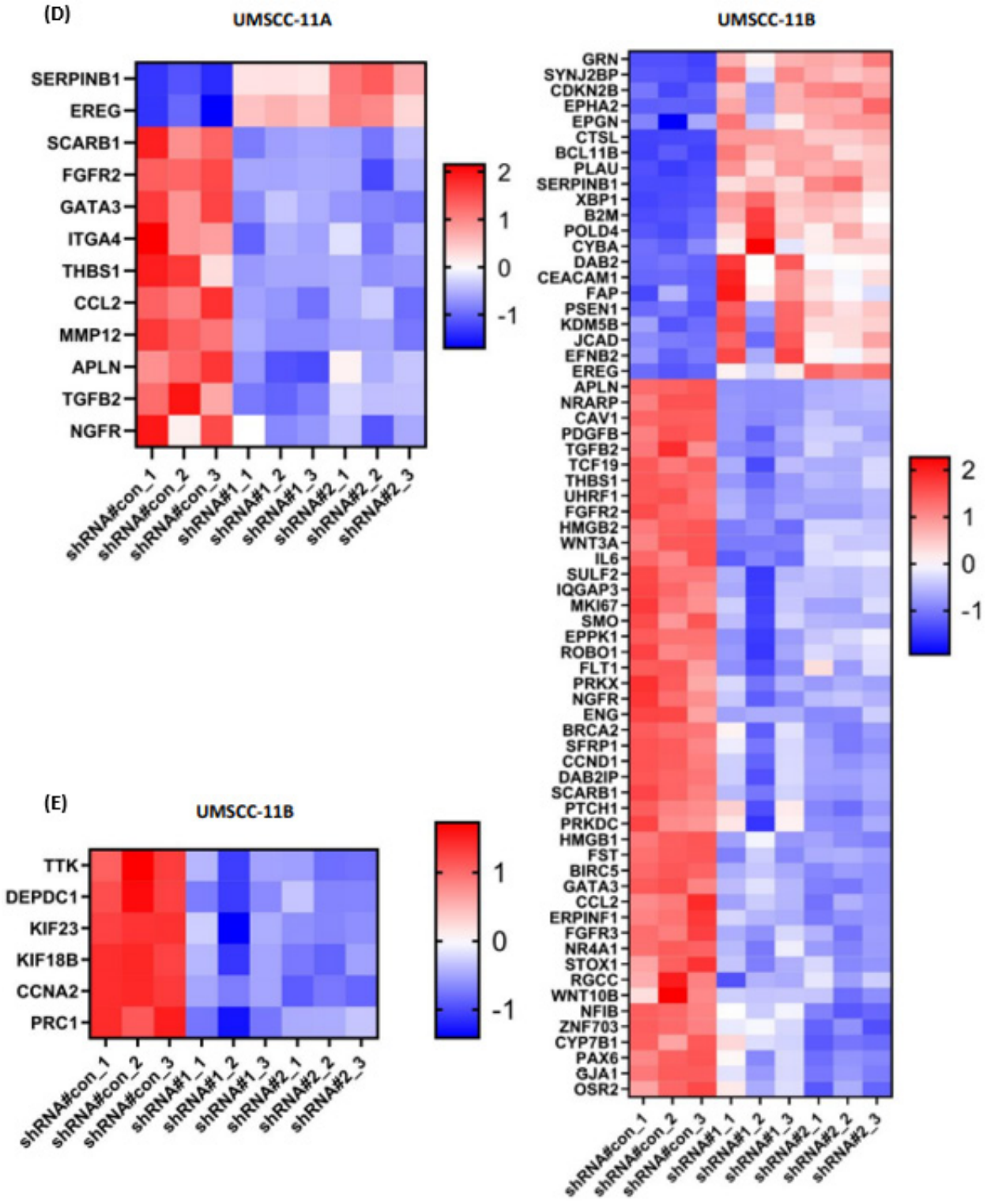
(D)
UMSCC-11A
SERPINB1
EREG
SCARB1
FGFR2
GATA3
ITGA4
THBS1
CCL2
MMP12
APLN
TGFB2
NGFR
shRNA#con_1
shRNA#con_2
shRNA#con_3
shRNA#1_1
shRNA#1_2
shRNA#1_3
shRNA#2_1
shRNA#2_2
shRNA#2_3
2
1
0
-1
UMSCC-11B
GRN
SYNJ2BP
CDKN2B
EPHA2
EPGN
CTSL
BCL11B
PLAU
SERPINB1
XBP1
B2M
POLD4
CYBA
DAB2
CEACAM1
FAP
PSEN1
KDM5B
JCAD
EFNB2
EREG
APLN
NRARP
CAV1
PDGFB
TGFB2
TCF19
THBS1
UHRF1
FGFR2
HMGB2
WNT3A
IL6
SULF2
IQGAP3
MKI67
SMO
EPPK1
ROBO1
FLT1
PRKX
NGFR
ENG
BRCA2
SFRP1
CCND1
DAB2IP
SCARB1
PTCH1
PRKDC
HMGB1
FST
BIRC5
GATA3
CCL2
ERPINF1
FGFR3
NR4A1
STOX1
RGCC
WNT10B
NFIB
ZNF703
CYP7B1
PAX6
GJA1
OSR2
shRNA#con_1
shRNA#con_2
shRNA#con_3
shRNA#1_1
shRNA#1_2
shRNA#1_3
shRNA#2_1
shRNA#2_2
shRNA#2_3
2
1
0
-1
(E)
UMSCC-11B
TTK
DEPDC1
KIF23
KIF18B
CCNA2
PRC1
shRNA#con_1
shRNA#con_2
shRNA#con_3
shRNA#1_1
shRNA#1_2
shRNA#1_3
shRNA#2_1
shRNA#2_2
shRNA#2_3
1
0
-1

(F)

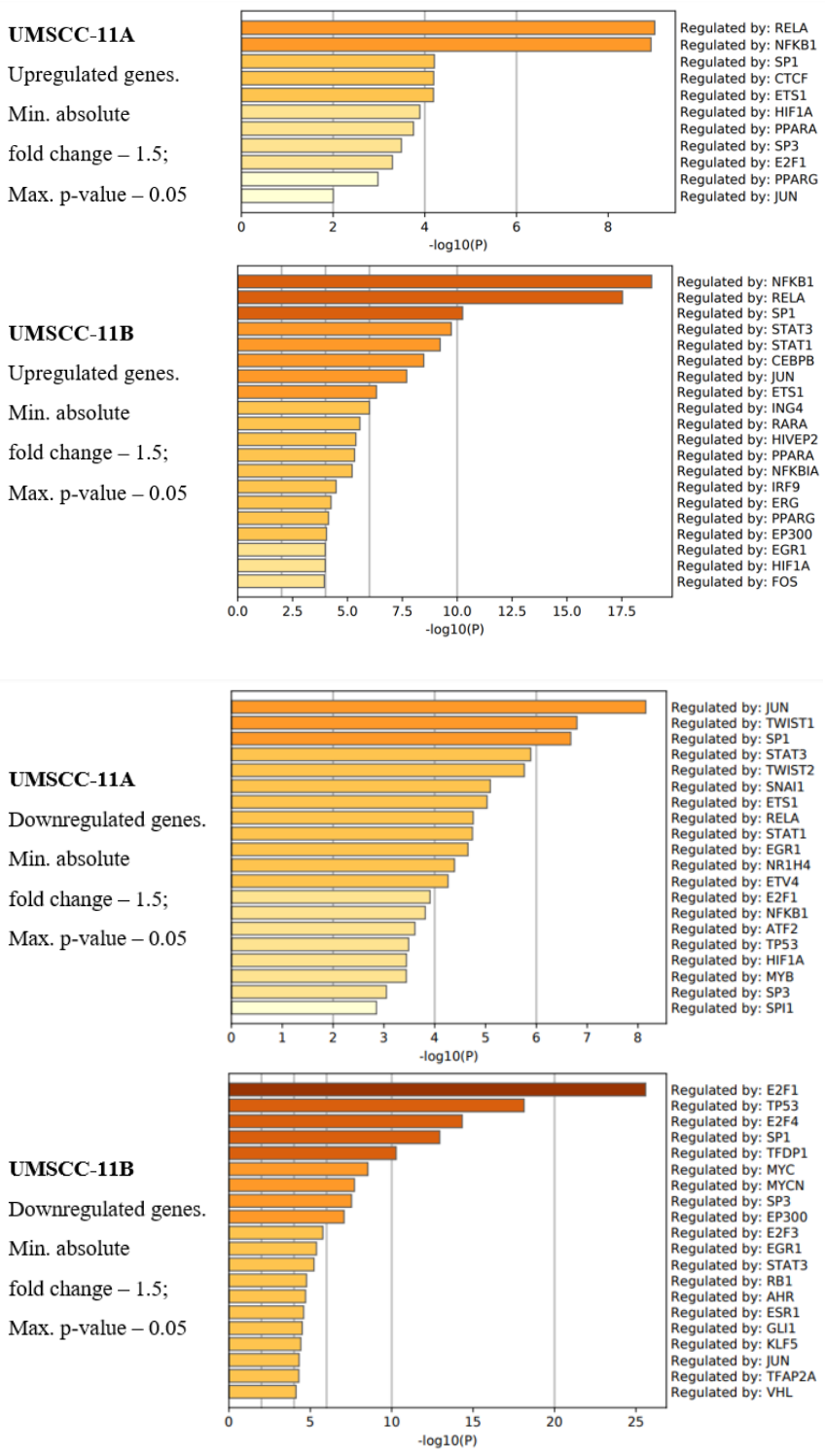

Figure 3.3. GPNMB knockdown-mediated downregulation of cellular proliferation, migration, and lymphovascular-invasion-related genes

(A) Principal component analysis illustrates distinction between control (red) and GPNMB KD (shRNA#1, green; shRNA#2, blue) clusters of samples. **(B)** Venn diagram illustrates shared, differentially expressed genes (DEGs) of two KD conditions (shRNA#1 and shRNA#2) compared to shRNA#control. **(C)** Heat map represents the DEGs profile of cellular migration-related genes. **(D)** Heat map represents the DEGs profile of cellular proliferation-related genes. **(E)** Heat map represents the DEGs profile of lymphovascular-invasion-related genes in UMSCC-11B. **(F)** Metascape (Zhou et al., 2019) analysis (GO_TRRUST) of DEGs in laryngeal UMSCC-11A, UMSCC-11B cell lines. Graphs represent most affected up- and down-regulated pathways through analysis of DEGs.

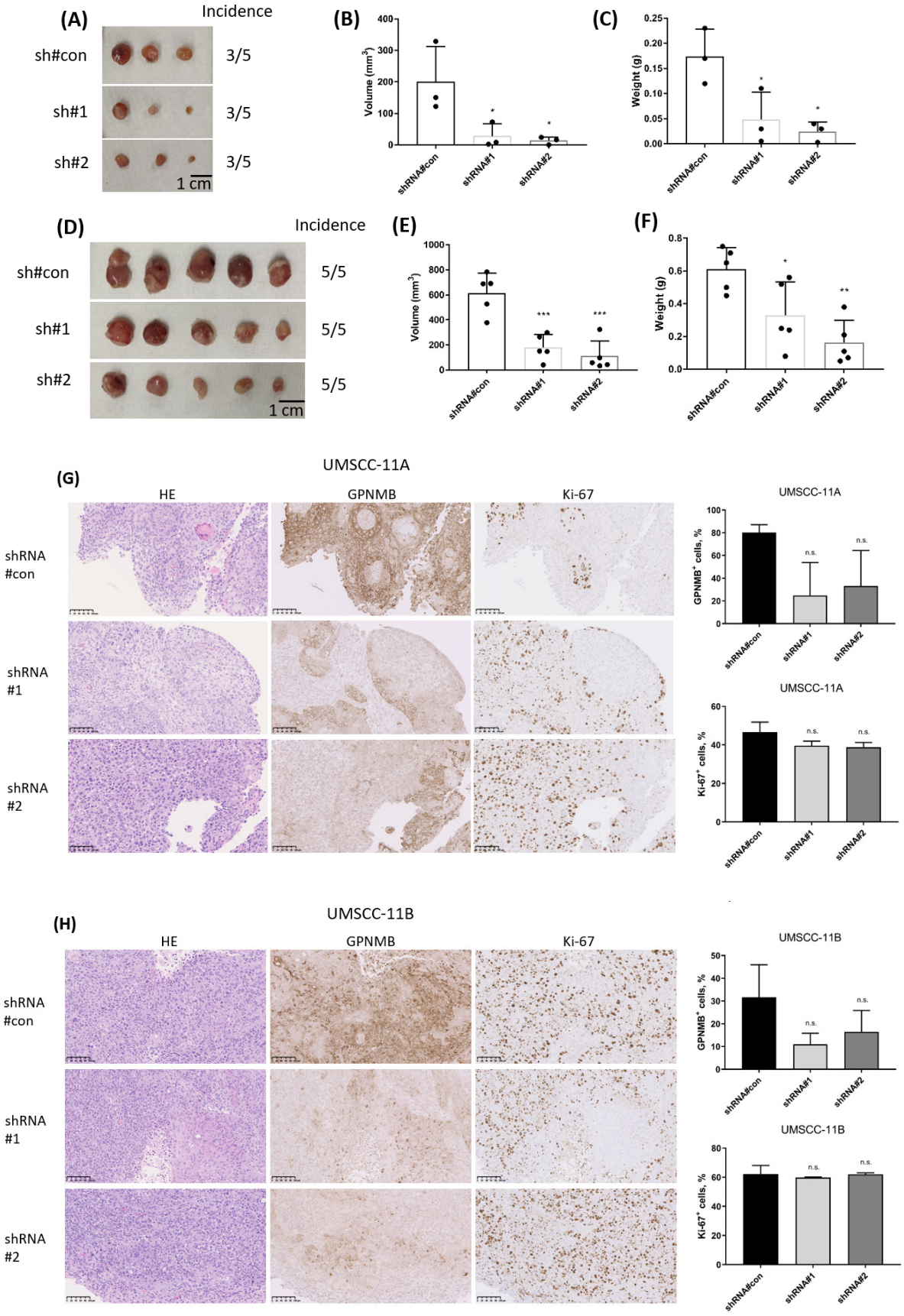
(A)
Incidence
sh#con
3/5
sh#1
3/5
sh#2
3/5
1 cm
(B)
Volume (mm3)
shRNA#con
shRNA#1
shRNA#2
(C)
Weight (g)
(D)
Incidence
sh#con
5/5
sh#1
5/5
sh#2
5/5
1 cm
(E)
Volume (mm3)
(F)
Weight (g)
(G)
UMSCC-11A
HE
GPNMB
Ki-67
shRNA #con
shRNA #1
shRNA #2
UMSCC-11A
GPNMB+ cells, %
Ki-67+ cells, %
n.s.
(H)
UMSCC-11B
HE
GPNMB
Ki-67
shRNA #con
shRNA #1
shRNA #2
UMSCC-11B
GPNMB+ cells, %
Ki-67+ cells, %

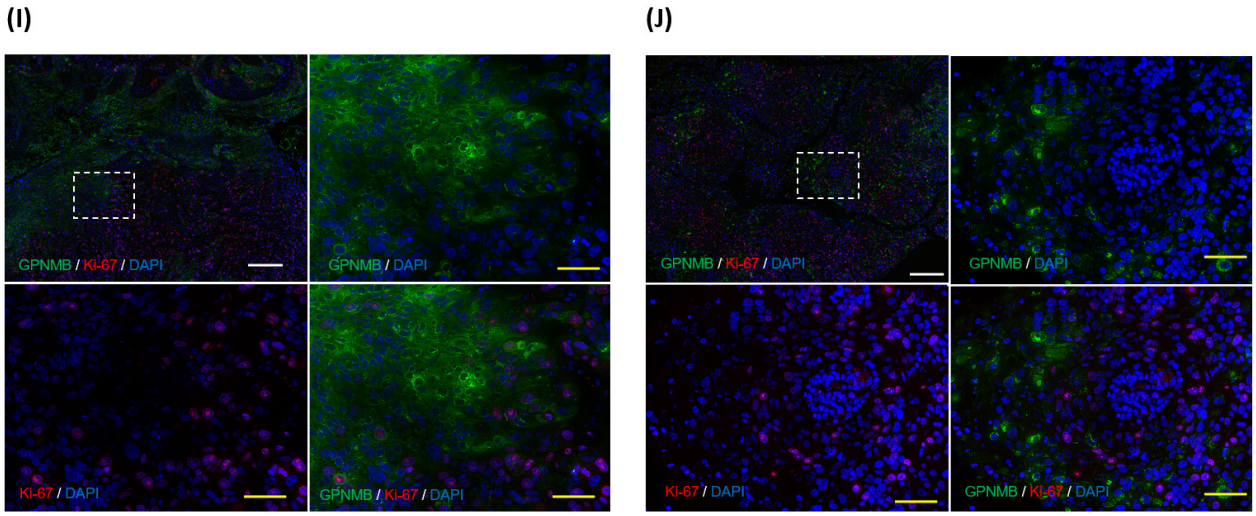

Figure 3.4. GPNMB regulates tumor formation *in vivo* in LSCC cell lines

(A-F) Tumor volumes and weights of UMSCC-11A (A-C) and of UMSCC-11B (D-F) with GPNMB KD subcutaneously injected cells into BALB/cAJcl-*nu/nu* mice. For A, D - incidence indicates the rate of tumor occurrence vs. the rate of subcutaneous injection. Data are presented as means ± SD. *$p < 0.05$, **$p < 0.01$, ***$p < 0.001$, one-way ANOVA with Tukey's multiple comparison test. **(G, H)** Hematoxylin and eosin (HE) staining of UMSCC-11A and -11B tumor sections, and immunohistochemical staining of GPNMB and Ki-67. Scale bars are 100 µm. Graphs represent detection of $GPNMB^+$ and $Ki\text{-}67^+$ cells within xenografted tumors based on QuPath analysis with single threshold of color intensity is 0.25. **(I, J)** Immunofluorescence staining of shRNA#con tumors from UMSCCC-11A and -11B with GPNMB (green), Ki-67 (red), and DAPI (blue). White scale bar is 200 µm, yellow scale bars are 50 µm.

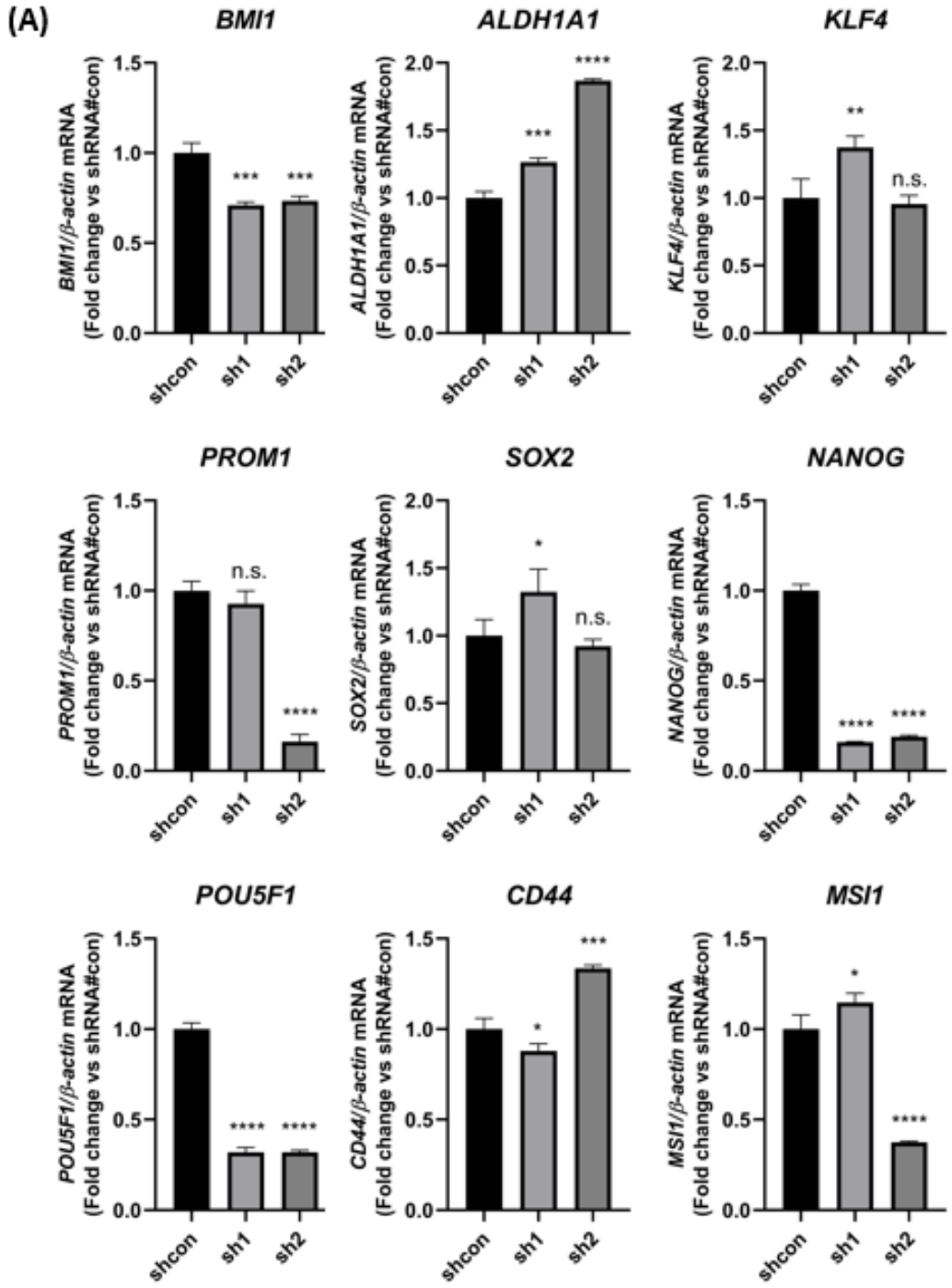
(A)
BMI1
ALDH1A1
KLF4
PROM1
SOX2
NANOG
POU5F1
CD44
MSI1
BMI1/β-actin mRNA (Fold change vs shRNA#con)
ALDH1A1/β-actin mRNA (Fold change vs shRNA#con)
KLF4/β-actin mRNA (Fold change vs shRNA#con)
PROM1/β-actin mRNA (Fold change vs shRNA#con)
SOX2/β-actin mRNA (Fold change vs shRNA#con)
NANOG/β-actin mRNA (Fold change vs shRNA#con)
POU5F1/β-actin mRNA (Fold change vs shRNA#con)
CD44/β-actin mRNA (Fold change vs shRNA#con)
MSI1/β-actin mRNA (Fold change vs shRNA#con)
shcon
sh1
sh2
n.s.

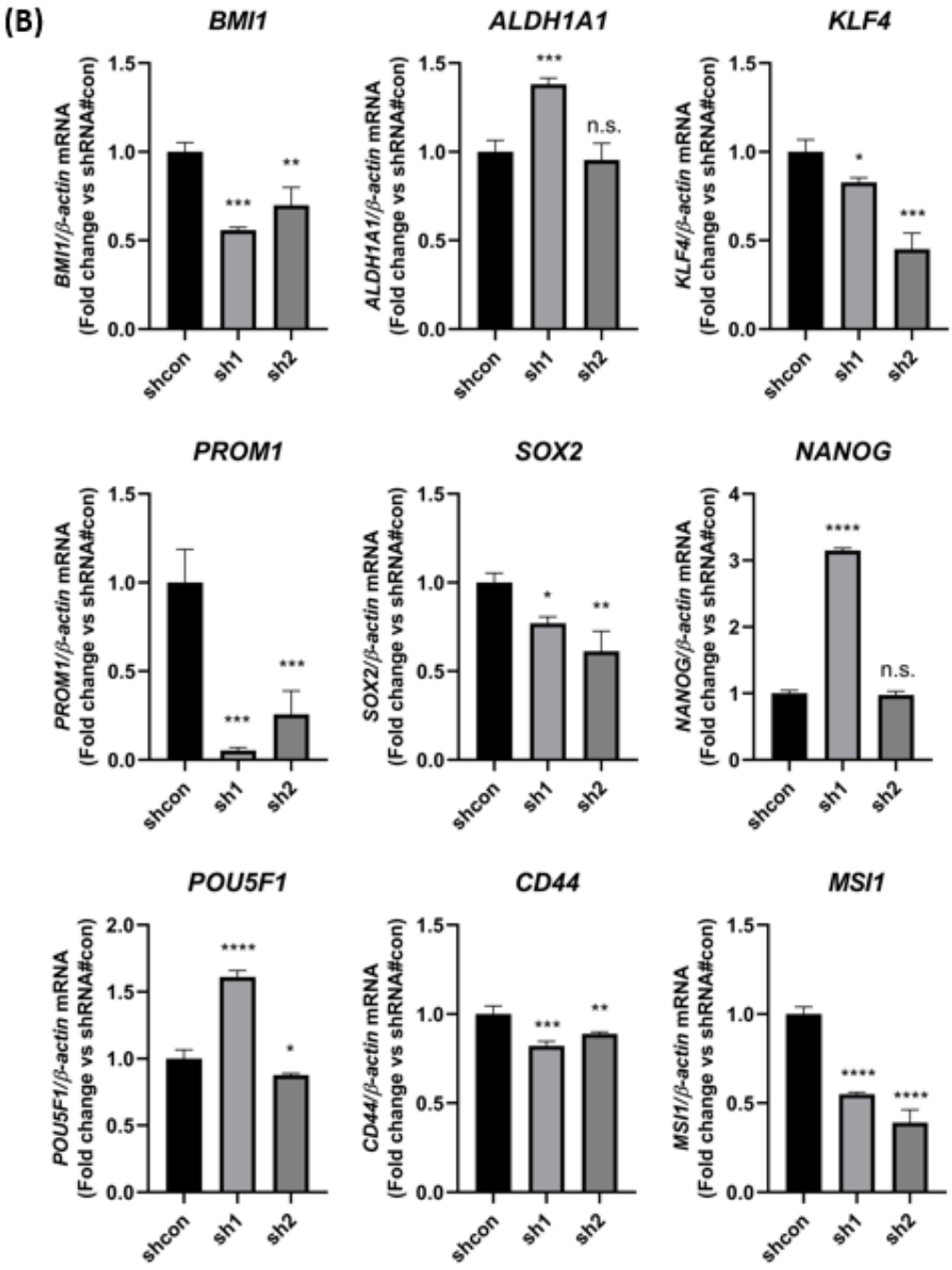

Figure 3.5. Expression of CSCs markers affected by GPNMB KD in UMSCC-11A (A) and UMSCC-11B (B) cells after sphere formation assay

Messenger RNA expression levels of *BMI1*, *ALDH1A1*, *KLF4*, *PROM1*, *SOX2*, *NANOG*, *POU5F1*, *CD44*, and *MSI1* in UMSCC-11B cell line were normalized to *β-actin*. Results are shown as means ± SD, representatives of triplicated experiments.

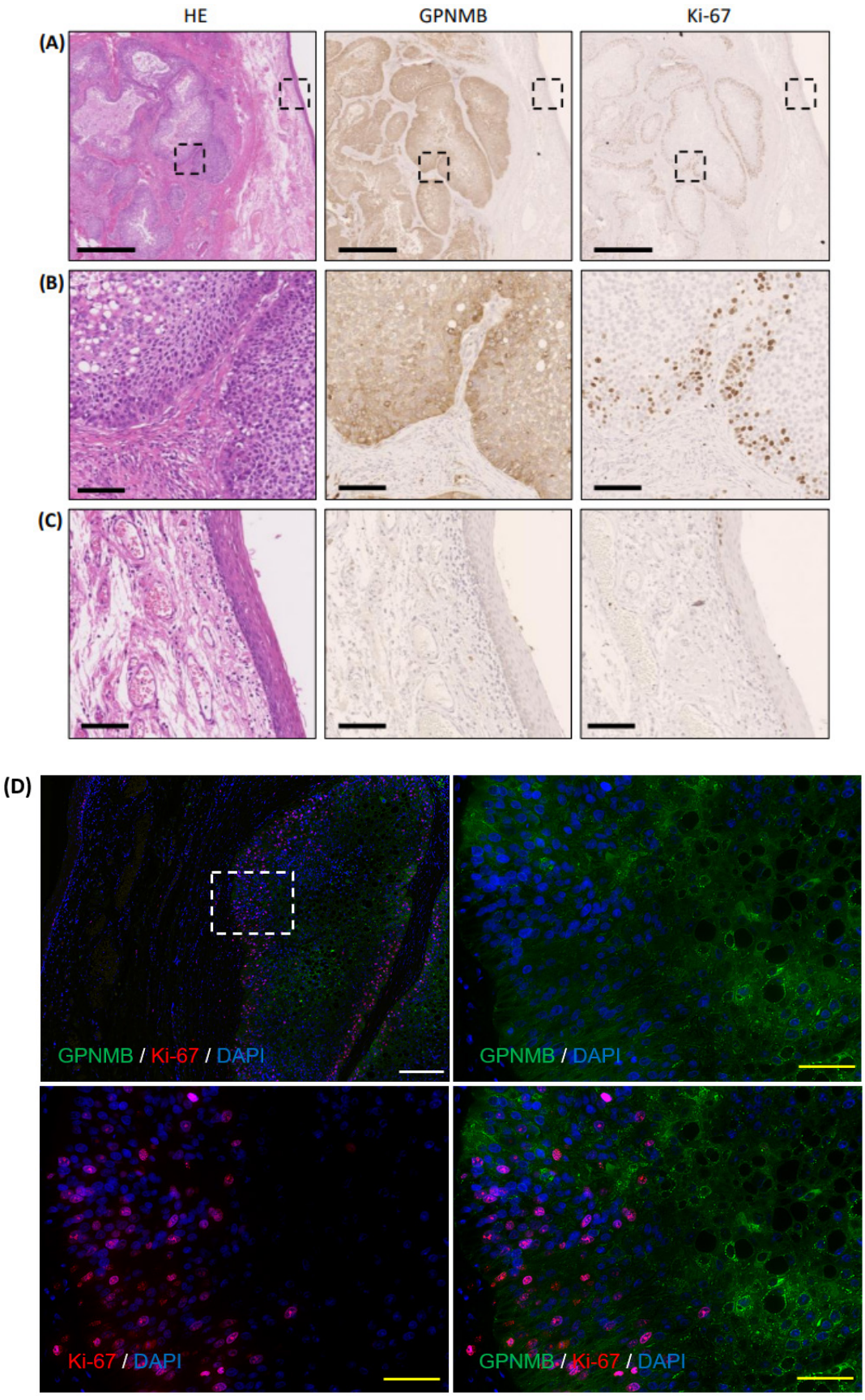
HE
GPNMB
Ki-67
(A)
(B)
(C)
(D)
GPNMB / Ki-67 / DAPI
GPNMB / DAPI
Ki-67 / DAPI
GPNMB / Ki-67 / DAPI

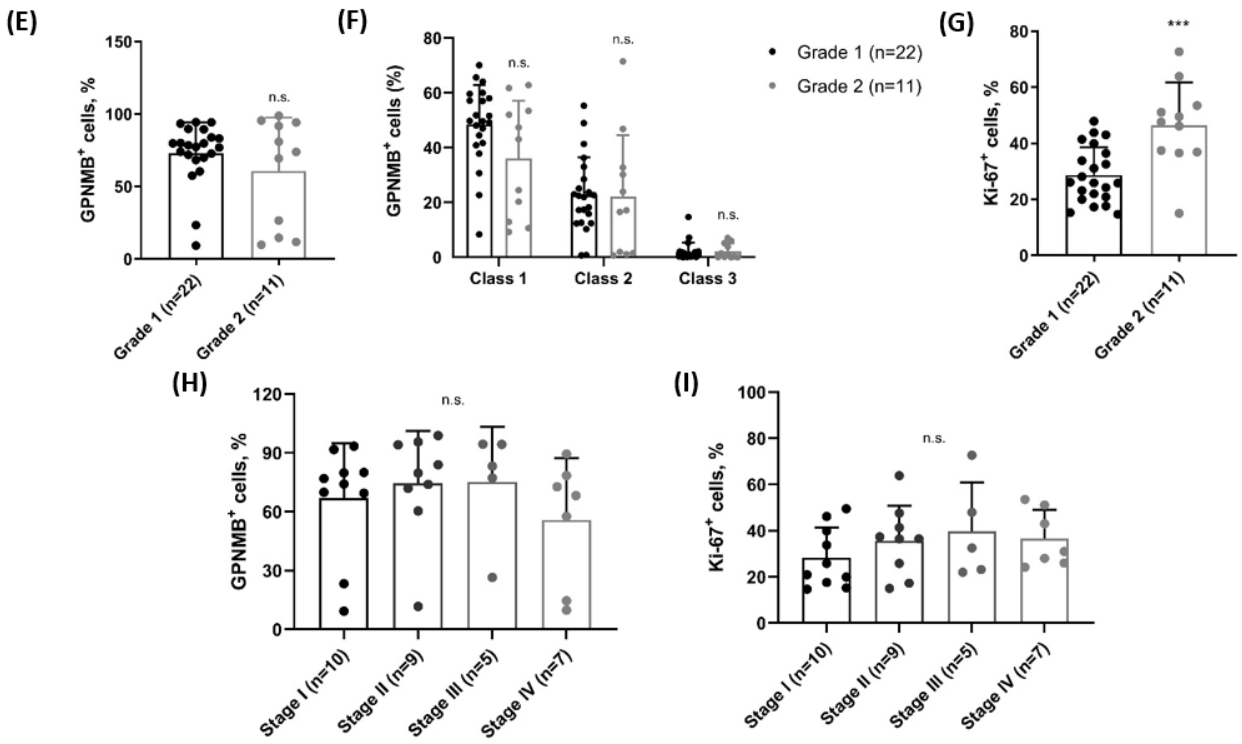

Figure 3.6. Expression of GPNMB and Ki-67 in tissue specimens of LSCC patients

(A) HE and IHC staining for GPNMB and Ki-67 in a representative clinical specimen. Scale bars are 1 mm. **(B, C)** The tumorous and normal epithelium of the clinical sample from the annotated areas in (A). Scale bars are 100 µm. **(D)** IF staining of a representative clinical specimen with GPNMB (green), Ki-67 (red), and DAPI (blue). White scale bar is 200 µm, yellow scale bars are 50 µm. (**E**) QuPath analysis of $GPNMB^+$ cells within laryngeal SCC specimens. Grade 1 stands for well-differentiated cases, Grade 2 – moderately-differentiated cases. Single threshold of color intensity is 0.25. (**F**) QuPath analysis of $GPNMB^+$ cells within laryngeal SCC specimens with multiple thresholds of color intensity. Class 1 represents the threshold at 0.25, Class 2 – at 0.4, Class 3 – at 0.6. (**G**) QuPath analysis of $Ki\text{-}67^+$ cells within laryngeal SCC specimens. Single threshold of color intensity is 0.25. (**H, I**) QuPath analysis of $GPNMB^+$ (H) and $Ki\text{-}67^+$ (I) cells within laryngeal SCC specimens compared to the clinical advancement. Single threshold of color intensity is 0.25.

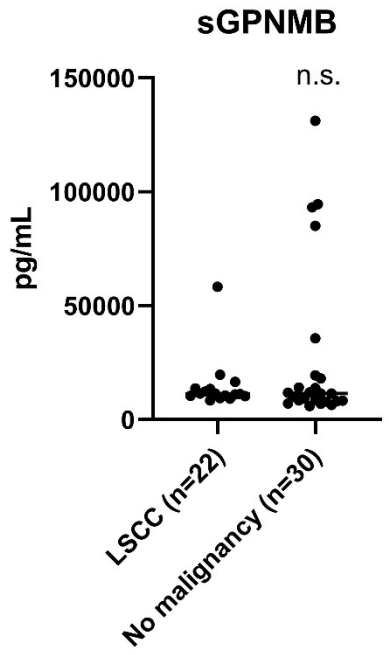

Figure 3.7. Concentrations of soluble GPNMB in serum samples of LSCC patients vs. control

The measurements represent the concentrations in both groups in pg/mL.

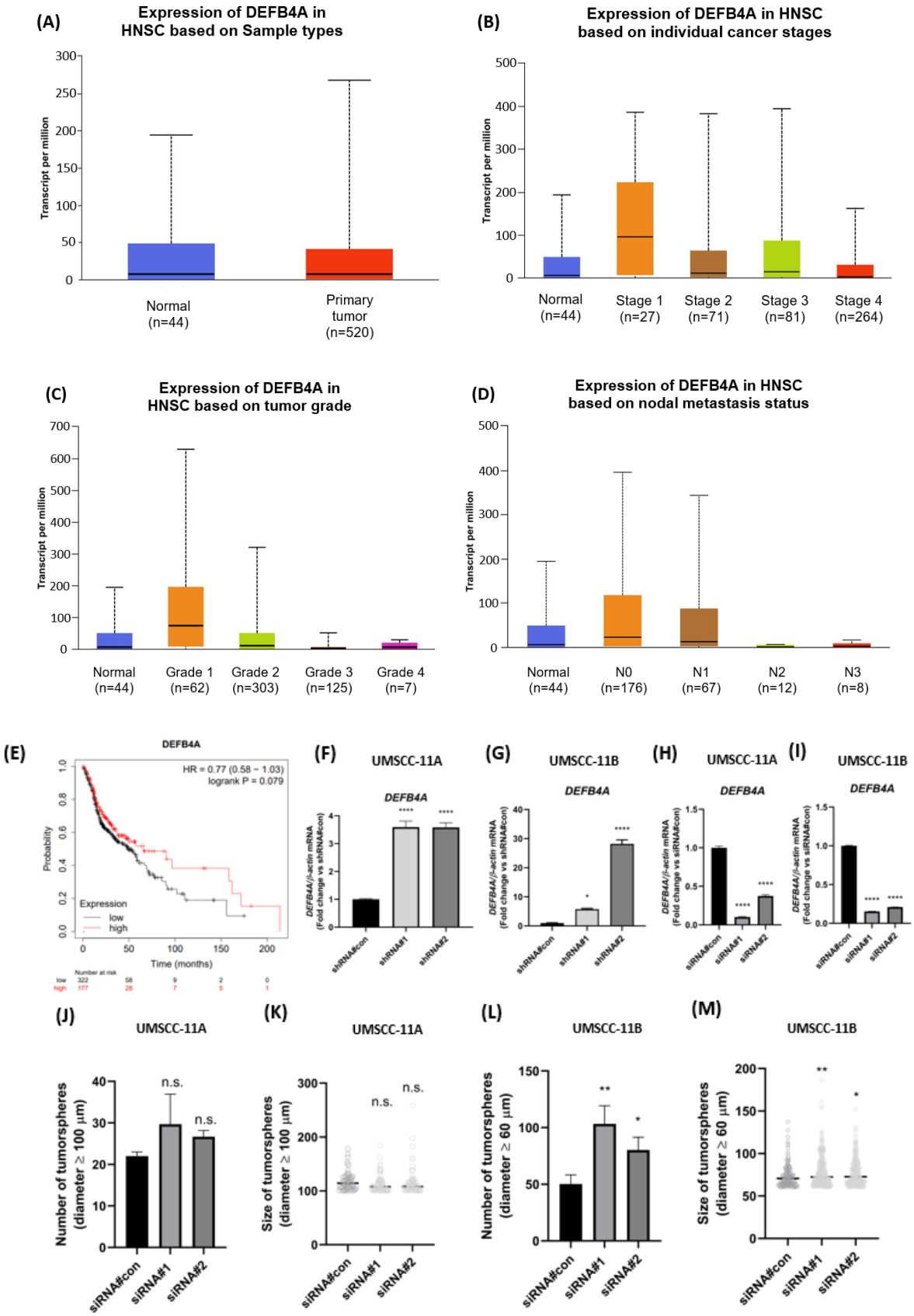
(A)
Expression of DEFB4A in HNSC based on Sample types
Transcript per million
Normal (n=44)
Primary tumor (n=520)
(B)
Expression of DEFB4A in HNSC based on individual cancer stages
Transcript per million
Normal (n=44)
Stage 1 (n=27)
Stage 2 (n=71)
Stage 3 (n=81)
Stage 4 (n=264)
(C)
Expression of DEFB4A in HNSC based on tumor grade
Transcript per million
Normal (n=44)
Grade 1 (n=62)
Grade 2 (n=303)
Grade 3 (n=125)
Grade 4 (n=7)
(D)
Expression of DEFB4A in HNSC based on nodal metastasis status
Transcript per million
Normal (n=44)
N0 (n=176)
N1 (n=67)
N2 (n=12)
N3 (n=8)
(E)
DEFB4A
HR = 0.77 (0.58 − 1.03)
logrank P = 0.079
Probability
Expression
low
high
Time (months)
Number at risk
(F)
UMSCC-11A
DEFB4A
(G)
UMSCC-11B
DEFB4A
(H)
UMSCC-11A
DEFB4A
(I)
UMSCC-11B
DEFB4A
shRNA#con
shRNA#1
shRNA#2
siRNA#con
siRNA#1
siRNA#2
(J)
UMSCC-11A
Number of tumorspheres (diameter ≥ 100 μm)
n.s.
(K)
UMSCC-11A
Size of tumorspheres (diameter ≥ 100 μm)
n.s.
(L)
UMSCC-11B
Number of tumorspheres (diameter ≥ 60 μm)
(M)
UMSCC-11B
Size of tumorspheres (diameter ≥ 60 μm)

Figure 3.8. DEFB4A role in HNSCC

(A) DEFB4A mRNA profile in primary head and neck squamous cell carcinoma (HNSC) specimens and normal specimens from the TCGA database (UALCAN analysis). **(B-D)** DEFB4A mRNA profile in primary HNSC specimens with different clinical stages, tumor grades and nodal metastasis status compared to normal specimens from the TCGA database. Respectively, grades 1 to 4 are defined as: well differentiated, moderately differentiated, poorly differentiated, undifferentiated subtypes. Nodal metastases are defined as: N0 – no regional lymph node metastasis, N1 – metastases in 1 to 3 axillary lymph nodes, N2 – metastases in 4 to 9 axillary lymph nodes, N3 – metastases in 10 or more axillary lymph nodes. **(E)** Overall Survival (OS) results of $DEFB4A^{high/low}$ in patients with HNSCC from Kaplan-Meier Plotter analysis. **(F, G)** GPNMB silencing-mediated upregulation of *DEFB4A* mRNA levels in UMSCC-11A and -11B. Expression levels were normalized to *β-actin*. **(H, I)** mRNA expression levels of *DEFB4A* affected by transient KD with small interference anti-DEFB4A mRNA in UMSCC-11A shRNA#2 and -11B shRNA#2 cell lines. Messenger RNA expression levels were normalized to *β-actin*. **(J-M)** Results indicate numbers and sizes of 3D spheres formed by UMSCC-11A shRNA#2, -11B shRNA#2 with siRNA-mediated DEFB4A KD. For UMSCC-11A shRNA#2 only spheres ≥ 100 μm in diameter were counted. For UMSCC-11B shRNA#2 only spheres ≥ 60 μm in diameter were counted. Results are shown as means ± SD, a representative of triplicated experiments.

Table 3.1. Statistical significance values of GPNMB in HSNCC cohort

Probability values of the Figure 3.1 A

* - the result is significant

Comparison	Statistical significance
*Normal-vs-Primary	1.62E-12

Probability values of the Figure 3.1 B

* - the result is significant

Comparison	Statistical significance
*Normal-vs-Stage 1	1.76E-04
*Normal-vs-Stage 2	9.04E-11
*Normal-vs-Stage 3	6.46E-09
*Normal-vs-Stage 4	<1E-12
Stage 1-vs-Stage 2	1.82E-01
*Stage 1-vs-Stage 3	4.65E-02
*Stage 1-vs-Stage 4	4.78E-03
Stage 2-vs-Stage 3	4.62E-01
Stage 2-vs-Stage 4	1.71E-01
Stage 3-vs-Stage 4	7.63E-01

Probability values of the Figure 3.1 C

* - the result is significant

Comparison	Statistical significance
*Normal-vs-Grade 1	1.37E-07
*Normal-vs-Grade 2	<1E-12
*Normal-vs-Grade 3	3.02E-13
*Normal-vs-Grade 4	4.08E-03
*Grade 1-vs-Grade 2	5.17E-04
Grade 1-vs-Grade 3	2.91E-01
*Grade 1-vs-Grade 4	1.26E-03
*Grade 2-vs-Grade 3	9.52E-03
Grade 2-vs-Grade 4	1.96E-01
*Grade 3-vs-Grade 4	1.56E-02

Table 3.3. Differentially Expressed Genes (DEGs) in UMSCC-11A, -11B.

Top 30 upregulated and downregulated genes in UMSCC-11A, -11B. The order of presented genes is based on their absolute fold change from highest to lowest.

Upregulated genes		Downregulated genes	
UMSCC-11A	**UMSCC-11B**	**UMSCC-11A**	**UMSCC-11B**
RPL17_C18orf32	AP003108.2	PINX1_1	AC005670.2
PCDHGA3	DEFB103B	GPNMB	MYOD1
PI3	EBF1	MXRA5	SOST
ARMCX5_GPRASP2	H2BS1	CCN5	PRICKLE4
MEFV	S100A12	C4B	PCDH19
VNN1	LCE3E	LRRC7	SLC1A6
IL13RA2	SIGLEC9	MMP12	SLAIN1
TREX1	TMEM238L	PTH1R	APLN
ANKRD22	RSAD2	AC008581.2	WNT3A
TCIM	TDRD9	CCL2	MGARP
LRRIQ1	EIF4EBP3	FN1	CSNK2A3
HSD17B2	CARD17	CGB3	KISS1R
ACOX2	IFNL1	CYP26A1	GPNMB
SPRR1B	IFI44L	CA9	ANKRD34B
RASGRP1	SAMSN1	CDH2	IGFL1
DEFB4A	LCE3D	PPARGC1A	SCARA3
TM4SF19	SERPIND1	DIO2	NEURL1B
S100A8	CLEC5A	KRT13	CCK

ANKRD33	MYCT1	ITGA4	MATN2
SERPINB2	PNLIPRP3	KANK4	CYFIP2
HBEGF	C11orf96	ZNF608	LZTS1
RP1	DEFB4A	CCN2	C4orf36
LCE3D	CALCR	MATN2	TMEM255A
S100A9	P2RY8	WNT5B	SERTAD4
RHCG	CEACAM6	PSG5	FBXO43
NTSR1	AKR1C1	APLN	MYLK
AC138969.1	SPRR1B	TBX10	KIF26A
CCL20	PI3	BCAM	NOX4
TIGD7	CMPK2	COMMD3_BMI1	UPK1B
KYNU	DEFB103A	EDIL3	RRM2

Table 3.8. Statistical significance values of DEFB4A in HSNCC cohort

Probability values of the Figure 3.8 A

No significant result

Comparison	Statistical significance
Normal-vs-Primary	5.68E-01

Probability values of the Figure 3.8 B

No significant result

Comparison	Statistical significance
Normal-vs-Stage 1	7.10E-01
Normal-vs-Stage 2	7.91E-01
Normal-vs-Stage 3	7.23E-01
Normal-vs-Stage 4	3.66E-01
Stage 1-vs-Stage 2	4.34E-01
Stage 1-vs-Stage 3	9.57E-01
Stage 1-vs-Stage 4	2.94E-01
Stage 2-vs-Stage 3	4.39E-01
Stage 2-vs-Stage 4	1.64E-01
Stage 3-vs-Stage 4	9.48E-02

Probability values of the Figure 3.8 C

* - the result is significant

Comparison	Statistical significance
Normal-vs-Grade 1	7.39E-01
Normal-vs-Grade 2	6.91E-01
Normal-vs-Grade 3	1.58E-01
Normal-vs-Grade 4	1.03E-01
Grade 1-vs-Grade 2	1.29E-01
*Grade 1-vs-Grade 3	1.63E-04
*Grade 1-vs-Grade 4	3.54E-05
*Grade 2-vs-Grade 3	3.21E-04
*Grade 2-vs-Grade 4	2.17E-05
Grade 3-vs-Grade 4	2.01E-01

Probability values of the Figure 3.8 D

* - the result is significant

Comparison	Statistical significance
Normal-vs-N0	8.85E-01
Normal-vs-N1	6.26E-01
Normal-vs-N2	1.32E-01
Normal-vs-N3	7.54E-02
N0-vs-N1	4.96E-01
*N0-vs-N2	1.3E-03
*N0-vs-N3	3.8E-05
*N1-vs-N2	1.2E-02
*N1-vs-N3	6.97E-04
N2-vs-N3	1.47E-01

CHAPTER 4. DISCUSSION

In this study, I presented the role of GPNMB as a key mediator of LSCC formation and progression. Being overexpressed in malignant cells, GPNMB regulates migration in 2D cultures, as well as proliferation in monolayer, anchorage-independent, and *in vivo* conditions. Glycoprotein NMB condition also affects expression profile of versatile pathways in cancer, resulting in differential expression of oncogenes and further malignant progression. GPNMB expression patterns correlate with the quiescent state of LSCC cells, suggesting that it participates in dormancy. Finally, in advanced LSCC, GPNMB could exhibit its negative regulation of DEFB4A, which later results in cancer progression.

The findings represent similar outcomes of hindered 2D cellular migration, 3D sphere formation *in vitro*, and tumor formation *in vivo* in LSCC during GPNMB silencing (Fig. 3.2 I-R; 3.4 A-F), as in previous studies with OSCC (Arosarena et al., 2016) or breast cancer (Okita et al., 2017). Although previous studies from our laboratory showed that GPNMB silencing does not restrain monolayer proliferation in 2D of breast cancer cell lines (Okita et al., 2017), it does impair cellular proliferation in the case of LSCC cell lines (Fig. 3.2 G, H). Thereby, the function of GPNMB ought to be diversified in different systems and organs; however, it is substantial for carcinogenesis in multiple cancer types.

The results from RNA-sequencing analysis have verified the importance of GPNMB in various LSCC tumorigenic processes. For instance, it was reported that simultaneously upregulated

TGFB2 and downregulated *DAB2* in HNSCC correlate with poor survival, cellular proliferation, and metastatic progression (Hannigan et al., 2010) while GPNMB silencing downregulates *TGFB2* gene in both LSCC cell lines and also upregulates *DAB*2 in UMSCC-11B (Fig. 3.3 C, D) to create a tumor suppressive microenvironment. Another crucial mediator of carcinogenic cellular processes is IL-6, which facilitates HNSCC progression and metastasis via lymphangiogenesis (Choudhary et al., 2016); while GPNMB KD significantly suppressed *IL6* expression in UMSCC-11B cell line, which was established from the post chemotherapeutic surgical site (Fig. 3.3 D). Furthermore, lymphangiogenesis was recognized as an underlying mechanism of lymph node metastasis in LSCC that worsens patient prognosis (Zhang et al., 2020). Zhang et al. reported six lymphovascular-invasion-related genes to be upregulated in SCC of head and neck; however, the stable GPNMB KD UMSCC-11B model presented decreased transcription of these genes (Fig. 3.3 E), exhibiting the uniqueness of glycoprotein NMB and its vast regulatory role in carcinogenesis of the larynx.

On the other hand, Ki-67 is a biomarker which denotes actively proliferating cells in G1, S, and G2 cell-cycle phases (Schrader et al., 2005). This marker serves as a prognostic factor during treatment for breast cancer (Soliman & Yussif, 2016), although its prognostic value was found to be indecisive in HNSCC patients using conventional treatment approaches (Chatzkel et al., 2017; Lavertu et al., 2001; Silva et al., 2004; Sittel et al., 2000). The evaluation of xenograft tumors formed from GPNMB KD and control cells did not exhibit significant differences in the ratio of Ki-67^{+} cells in the tumors (Fig. 3.4 G, H). Nevertheless, a significant impairment in tumor formation was attained from GPNMB-depleted cells (Fig. 3.4 A-F). Consequently, Ki-67 status

cannot be a representative biomarker of carcinogenic activity changes with regard to GPNMB, at least within *in vivo* tumor models.

In addition, I have revealed that GPNMB$^+$ cells primarily do not express nuclear Ki-67, an inverse relationship that seems solid (Fig. 3.4 I, J; 3.6 D) and directive that GPNMB$^+$ cells are in non-proliferating state in LSCC. Moreover, recent scientific studies have contributed to the theory that cancer stem cells (CSCs) are involved in cancer dormancy, drug resistance, relapse, and further carcinogenesis (Ayob & Ramasamy, 2018; Najafi et al., 2019; Yang et al., 2020). Previous works from our group have confirmed the involvement of GPNMB exposed on the cell surface in onset and sustenance of CSCs in breast cancer cell lines (Chen et al., 2018). Thereby, I suggest that the GPNMB$^+$/Ki-67$^-$ cells are a population of cancer stem-like cells in LSCC. To examine this possibility, I assessed the expression of nine CSC-related genes (Fig. 3.5). As for now, I could confirm that GPNMB KD suppressed *BMI1* expression in both primary and advanced representatives of laryngeal SCC. *BMI1* is a target gene of E2F1 pathway (Nowak, 2006). Interestingly, among most downregulated genes in both cell-lines (Fig. 3.3 F), there were presented numerous target genes dependent on E2F1. Based on these expression patterns, I suggest that GPNMB KD reduces the activity of E2F1, partially resulting in suppression of self-renewal ability, proliferation, and migration (Meng & Ghosh, 2014). However, expression of other 8 CSC-related genes was inconsistent between knockdown conditions as well as between cell-lines (Fig. 3.5). One of the reports suggests the existence of several subpopulations of CSCs in HNSCC, while *POU5F1* (OCT4), *SOX2*, and *PROM1* (CD133) were not expressed consistently (Han et al., 2014). Besides, GPNMB might explicit different capabilities among primary and advanced types of cancer. Therefore, it is necessary to further investigate the expression patterns of CSCs markers in other laryngeal representatives, including primary and metastatic derivatives. These findings

suggest that GPNMB is partially involved in the regulation of CSC populations in LSCC and it has yet to be fully elucidated.

GPNMB has a potential to be cleaved by such metalloproteinase (MMP), as ADAM 10 (Rose et al., 2010), and explicit various functions, including tumorigenic or metabolic properties locally and systemically (Gong et al., 2019; Liguori et al., 2021). There were reports in which serum levels of sGPNMB might serve as a marker for classification between resistant types of non-small cell lung carcinoma (Chung et al., 2019). As such, I hypothesized that the presence of sGPNMB in a systemic blood circulation can be a supplementary marker for SCC clinical diagnosis. However, the results represented that low and high concentrations of soluble GPNMB were measured in both non-malignant and LSCC cases (Fig. 3.7). This outcome suggests that sGPNMB might be not a unique and suitable marker for laryngeal SCC diagnosis.

Among most upregulated genes I have found several defensins to be dramatically increased in GPNMB KD samples compared to control (Table 3.3). Among those, lower expression of *DEFB4A* significantly correlated with the progression of advanced HNSCC according to TCGA database (Fig. 3.8 C, D). As *DEFB4A* expression is regulated by activation of NF-κB, GPNMB KD resulted in significant upregulation of the NF-κB/RELA pathway (Fig. 3.3 F). According to Wang et al. (Wang & Tatakis, 2018), cohort of smoking patients exhibited significantly downregulated *DEFB4A* from palatal biopsies, compared to non-smoking cohort; whereas smoking is considered to be a crucial risk factor for carcinogenesis of HNSCC. Among few published reports up to date, confirming the DEFB4A involvement in tumorigenesis, higher expression of DEFB4A was associated with migration in colorectal cancer (Wu et al., 2020) and with invasion in esophageal SCC (Shi et al., 2014). In opposite, OSCC was associated with loss

of β-defensins as HBD-1, HBD-2 (DEFB4A), and HBD-3 (Joly et al., 2009). Interestingly, within my models, *DEFB4A* expression pattern and functionality between two cell lines appeared to be different. While strongly upregulated in parental and GPNMB KD conditions in UMSCC-11B, silencing of DEFB4A could result in significant recovery of 3D sphere forming ability. Mostly, β-defensins are reported to be antibacterial molecules, where DEFB4A forms a positively-charged octamer and makes pores in anionic bacterial cell walls (Hoover et al., 2000); however, some reports show the function of DEFB4A as a ligand for CCR6 chemokine receptor presented on immune cells (Koeninger et al., 2020) as well as on metastatic HNSCC cells (Wang et al., 2004). CCR6 presence was related to more advanced/metastatic LSCC progression (Chen et al., 2013). Nevertheless, GPNMB KD-mediated abundant expression of DEFB4A within this mechanism could abrogate tumor sphere formation in my model of the advanced LSCC cell line. Therefore, I hypothesize that GPNMB promotes malignant progression of advanced or metastatic LSCC through downregulation of DEFB4A expression. Whether GPNMB regulates this downstream directly or indirectly is yet to be understood.

CHAPTER 5. CONCLUSION

Recent discoveries in molecular biology, evolution of precision medicine, and advancements in surgery have improved the care for patients diagnosed with cancer leading them to have less possible side effects, organ-preserving solutions, and increased quality of life. Nevertheless, laryngeal squamous cell carcinoma, as a part of HNSCC, remains to be heterogeneous in nature, highly treatment-resistant, and life-threatening disease. Until now total laryngectomy continues to be a frequent approach in advanced cases, while patients tackle the consequences of dysphonia. In other common scenarios, patients have to compromise with the outcomes of as saving as disabling chemotherapy. Precise medicine remains to be in embryonic state until now, with understandably slow and extremely expensive clinical trials. To increase the chances of effective and safe treatment there is a need to investigate mechanisms underlying the causes of initiation, progression, or relapse of the cancer. This study shows glycoprotein NMB as a unique oncogene within LSCC. One of the interesting features lies within the outcome, that GPNMB regulates proliferation in 2D and 3D, however, is expressed in non-proliferative cells. GPNMB expression was not in correlation with the clinical progression of LSCC within our cohort and the protein levels were decreased in more advanced cell lines, like UMSCC-10B, -11B, over UMSCC-10A, -11A, albeit in such an advanced representative as UMSCC-11B, it could significantly regulate the expression of DEFB4A, which under suppression lost such anti-tumorigenic function, as inhibition of 3D sphere formation. UMSCC-11A and -11B were derived from the same patient, although, RNA-sequencing results showed the different gene signature during the GPNMB KD experiments, thus it confirms the heterogeneous nature of LSCC. Finally, CSCs populations were affected in different manner, suggesting that GPNMB can play versatile roles in dissimilar origins of LSCC.

Since there are few reports on the GPNMB involvement in HNSCC present up to date, my work shows the importance of GPNMB functionality and correlation within LSCC progression, suggests its involvement in regulation of CSCs population and partially discovers a novel mechanism of GPNMB – DEFB4A axis. As such, I suggest GPNMB as a diagnostic marker for surgically obtained specimens and as a novel therapeutic target within LSCC patients.

CHAPTER 6. GRAPHICAL SUMMARY

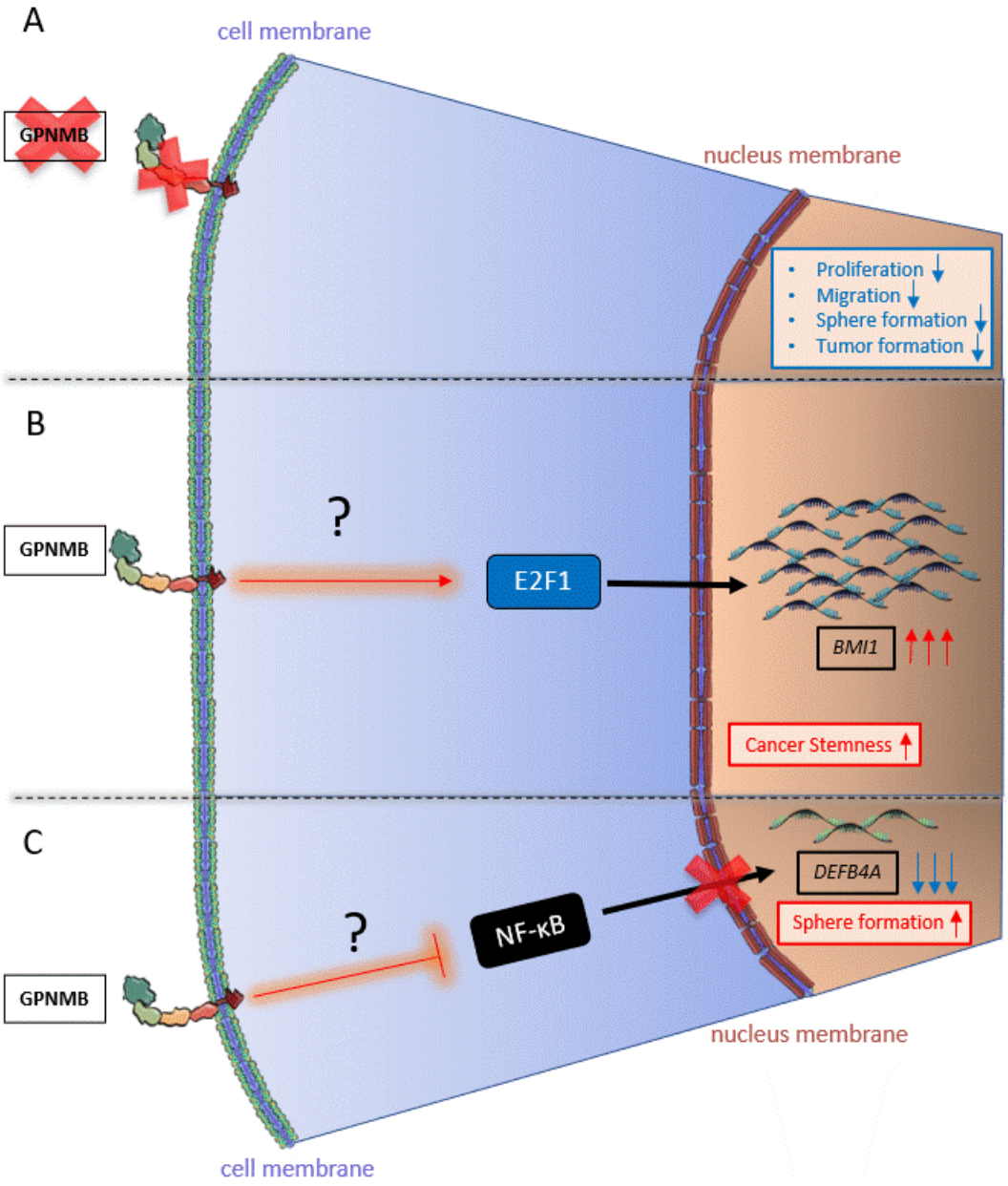

A. GPNMB knockdown reduces LSCC progression

B. GPNMB partially promotes cancer stemness properties of LSCC via *BMI1* upregulation

C. GPNMB induces malignant progression of advanced LSCC through *DEFB4A* inhibition

REFERENCES

Abdelmagid, S. M., Barbe, M. F., Arango-Hisijara, I., Owen, T. A., Popoff, S. N., & Safadi, F. F. (2007). Osteoactivin acts as downstream mediator of BMP-2 effects on osteoblast function. *Journal of Cellular Physiology*, *210*(1), 26–37. https://doi.org/10.1002/jcp.20841

Abdelmagid, S. M., Barbe, M. F., Hadjiargyrou, M., Owen, T. A., Razmpour, R., Rehman, S., Popoff, S. N., & Safadi, F. F. (2010). Temporal and spatial expression of osteoactivin during fracture repair. *Journal of Cellular Biochemistry*, *111*(2), 295–309. https://doi.org/10.1002/jcb.22702

Agrawal, N., Frederick, M. J., Pickering, C. R., Bettegowda, C., Chang, K., Li, R. J., Fakhry, C., Xie, T.-X., Zhang, J., Wang, J., Zhang, N., El-Naggar, A. K., Jasser, S. A., Weinstein, J. N., Treviño, L., Drummond, J. A., Muzny, D. M., Wu, Y., Wood, L. D., … Myers, J. N. (2011). Exome Sequencing of Head and Neck Squamous Cell Carcinoma Reveals Inactivating Mutations in NOTCH1. *Science*, *333*(6046), 1154–1157. https://doi.org/10.1126/science.1206923

Al-Hajj, M., Wicha, M. S., Benito-Hernandez, A., Morrison, S. J., & Clarke, M. F. (2003). Prospective identification of tumorigenic breast cancer cells. *Proceedings of the National Academy of Sciences*, *100*(7), 3983–3988. https://doi.org/10.1073/pnas.0530291100

Alsahafi, E., Begg, K., Amelio, I., Raulf, N., Lucarelli, P., Sauter, T., & Tavassoli, M. (2019). Clinical update on head and neck cancer: molecular biology and ongoing challenges. *Cell Death & Disease*, *10*(8), 540. https://doi.org/10.1038/s41419-019-1769-9

Arosarena, O. A., Barr, E. W., Thorpe, R., Yankey, H., Tarr, J. T., & Safadi, F. F. (2018). Osteoactivin regulates head and neck squamous cell carcinoma invasion by modulating matrix metalloproteases. *Journal of Cellular Physiology*, *233*(1), 409–421.

https://doi.org/10.1002/jcp.25900

Arosarena, O. A., dela Cadena, R. A., Denny, M. F., Bryant, E., Barr, E. W., Thorpe, R., & Safadi, F. F. (2016). Osteoactivin Promotes Migration of Oral Squamous Cell Carcinomas. *Journal of Cellular Physiology*, *231*(8), 1761–1770. https://doi.org/10.1002/jcp.25279

Ayob, A. Z., & Ramasamy, T. S. (2018). Cancer stem cells as key drivers of tumour progression. *Journal of Biomedical Science*, *25*(1), 20. https://doi.org/10.1186/s12929-018-0426-4

Bankhead, P., Loughrey, M. B., Fernández, J. A., Dombrowski, Y., McArt, D. G., Dunne, P. D., McQuaid, S., Gray, R. T., Murray, L. J., Coleman, H. G., James, J. A., Salto-Tellez, M., & Hamilton, P. W. (2017). QuPath: Open source software for digital pathology image analysis. *Scientific Reports*, *7*(1), 16878. https://doi.org/10.1038/s41598-017-17204-5

Baselga, J. (2002). Why the Epidermal Growth Factor Receptor? The Rationale for Cancer Therapy. *The Oncologist*, *7*(S4), 2–8. https://doi.org/10.1634/theoncologist.7-suppl_4-2

Bonnet, D., & Dick, J. E. (1997). Human acute myeloid leukemia is organized as a hierarchy that originates from a primitive hematopoietic cell. *Nature Medicine*, *3*(7), 730–737. https://doi.org/10.1038/nm0797-730

Bradford, C. R., Zhu, S., Poore, J., Fisher, S. G., Beals, T. F., Thoraval, D., Hanash, S. M., Carey, T. E., & Wolf, G. T. (1997). p53 Mutation as a Prognostic Marker in Advanced Laryngeal Carcinoma. *Archives of Otolaryngology - Head and Neck Surgery*, *123*(6), 605–609. https://doi.org/10.1001/archotol.1997.01900060047008

Braig, F., Kriegs, M., Voigtlaender, M., Habel, B., Grob, T., Biskup, K., Blanchard, V., Sack, M., Thalhammer, A., Ben Batalla, I., Braren, I., Laban, S., Danielczyk, A., Goletz, S., Jakubowicz, E., Märkl, B., Trepel, M., Knecht, R., Riecken, K., … Binder, M. (2017). Cetuximab Resistance in Head and Neck Cancer Is Mediated by EGFR-K 521

Polymorphism. *Cancer Research*, *77*(5), 1188–1199. https://doi.org/10.1158/0008-5472.CAN-16-0754

Brenner, J. C., Graham, M. P., Kumar, B., Saunders, L. M., Kupfer, R., Lyons, R. H., Bradford, C. R., & Carey, T. E. (2010). Genotyping of 73 UM-SCC head and neck squamous cell carcinoma cell lines. *Head & Neck*, *32*(4), 417–426. https://doi.org/10.1002/hed.21198

Burtness, B., Goldwasser, M. A., Flood, W., Mattar, B., Forastiere, A. A., & Eastern Cooperative Oncology Group. (2005). Phase III randomized trial of cisplatin plus placebo compared with cisplatin plus cetuximab in metastatic/recurrent head and neck cancer: an Eastern Cooperative Oncology Group study. *Journal of Clinical Oncology : Official Journal of the American Society of Clinical Oncology*, *23*(34), 8646–8654. https://doi.org/10.1200/JCO.2005.02.4646

Chandrashekar, D. S., Bashel, B., Balasubramanya, S. A. H., Creighton, C. J., Ponce-Rodriguez, I., Chakravarthi, B. V. S. K., & Varambally, S. (2017). UALCAN: A Portal for Facilitating Tumor Subgroup Gene Expression and Survival Analyses. *Neoplasia (New York, N.Y.)*, *19*(8), 649–658. https://doi.org/10.1016/j.neo.2017.05.002

Chatzkel, J., Lewis, J. S., Ley, J. C., Wildes, T. M., Thorstad, W., Gay, H., Daly, M., Jackson, R., Rich, J., Paniello, R., Nussenbaum, B., Liu, J., Siegel, B. A., Dehdashti, F., & Adkins, D. (2017). Correlation of Ki-67 Proliferative Antigen Expression and Tumor Response to Induction Chemotherapy Containing Cell Cycle-Specific Agents in Head and Neck Squamous Cell Carcinoma. *Head and Neck Pathology*, *11*(3), 338–345. https://doi.org/10.1007/s12105-016-0775-9

Chen, B., Zhang, D., Zhou, J., Li, Q., Zhou, L., Li, S.-M., Zhu, L., Chou, K.-Y., Zhou, L., Tao, L., & Lu, L.-M. (2013). High CCR6/CCR7 expression and Foxp3+ Treg cell number are

positively related to the progression of laryngeal squamous cell carcinoma. *Oncology Reports*, *30*(3), 1380–1390. https://doi.org/10.3892/or.2013.2603

Chen, C., Okita, Y., Watanabe, Y., Abe, F., Fikry, M. A., Ichikawa, Y., Suzuki, H., Shibuya, A., & Kato, M. (2018). Glycoprotein nmb Is Exposed on the Surface of Dormant Breast Cancer Cells and Induces Stem Cell–like Properties. *Cancer Research*, *78*(22), 6424–6435. https://doi.org/10.1158/0008-5472.CAN-18-0599

Choudhary, M. M., France, T. J., Teknos, T. N., & Kumar, P. (2016). Interleukin-6 role in head and neck squamous cell carcinoma progression. *World Journal of Otorhinolaryngology - Head and Neck Surgery*, *2*(2), 90–97. https://doi.org/10.1016/j.wjorl.2016.05.002

Chung, J.-S., Bonkobara, M., Tomihari, M., Cruz, P. D., & Ariizumi, K. (2009). The DC-HIL/syndecan-4 pathway inhibits human allogeneic T-cell responses. *European Journal of Immunology*, *39*(4), 965–974. https://doi.org/10.1002/eji.200838990

Chung, J.-S., Ramani, V., Kobayashi, M., Popat, V., Cruz, P. D., Gerber, D. E., & Ariizumi, K. (2019). Expression of soluble DC-HIL/gpnmb receptor in the blood of metastatic non-small cell lung carcinoma treated with anti-PD1/PDL1 monoclonal antibodies. *Journal of Clinical Oncology*, *37*(15_suppl), e14038–e14038. https://doi.org/10.1200/JCO.2019.37.15_suppl.e14038

Clarke, M. F., Dick, J. E., Dirks, P. B., Eaves, C. J., Jamieson, C. H. M., Jones, D. L., Visvader, J., Weissman, I. L., & Wahl, G. M. (2006). Cancer Stem Cells—Perspectives on Current Status and Future Directions: AACR Workshop on Cancer Stem Cells. *Cancer Research*, *66*(19), 9339–9344. https://doi.org/10.1158/0008-5472.CAN-06-3126

Cooper, J. S., Pajak, T. F., Forastiere, A. A., Jacobs, J., Campbell, B. H., Saxman, S. B., Kish, J. A., Kim, H. E., Cmelak, A. J., Rotman, M., Machtay, M., Ensley, J. F., Chao, K. S. C.,

Schultz, C. J., Lee, N., & Fu, K. K. (2004). Postoperative Concurrent Radiotherapy and Chemotherapy for High-Risk Squamous-Cell Carcinoma of the Head and Neck. *New England Journal of Medicine*, *350*(19), 1937–1944. https://doi.org/10.1056/NEJMoa032646

Department of Veterans Affairs Laryngeal Cancer Study Group, Wolf, G. T., Fisher, S. G., Hong, W. K., Hillman, R., Spaulding, M., Laramore, G. E., Endicott, J. W., McClatchey, K., & Henderson, W. G. (1991). Induction chemotherapy plus radiation compared with surgery plus radiation in patients with advanced laryngeal cancer. *The New England Journal of Medicine*, *324*(24), 1685–1690. https://doi.org/10.1056/NEJM199106133242402

Dotto, G. P. (2008). Notch tumor suppressor function. *Oncogene*, *27*(38), 5115–5123. https://doi.org/10.1038/onc.2008.225

Fattizzo, B., Rosa, J., Giannotta, J. A., Baldini, L., & Fracchiolla, N. S. (2020). The Physiopathology of T- Cell Acute Lymphoblastic Leukemia: Focus on Molecular Aspects. *Frontiers in Oncology*, *10*. https://doi.org/10.3389/fonc.2020.00273

Ferlay, J., Colombet, M., Soerjomataram, I., Parkin, D. M., Piñeros, M., Znaor, A., & Bray, F. (2021). Cancer statistics for the year 2020: An overview. *International Journal of Cancer*, *149*(4), 778–789. https://doi.org/10.1002/ijc.33588

Forastiere, A. A., Goepfert, H., Maor, M., Pajak, T. F., Weber, R., Morrison, W., Glisson, B., Trotti, A., Ridge, J. A., Chao, C., Peters, G., Lee, D.-J., Leaf, A., Ensley, J., & Cooper, J. (2003). Concurrent Chemotherapy and Radiotherapy for Organ Preservation in Advanced Laryngeal Cancer. *New England Journal of Medicine*, *349*(22), 2091–2098. https://doi.org/10.1056/NEJMoa031317

Fukusumi, T., & Califano, J. A. (2018). The NOTCH Pathway in Head and Neck Squamous Cell Carcinoma. *Journal of Dental Research*, *97*(6), 645–653.

https://doi.org/10.1177/0022034518760297

Geiger, J. L., Grandis, J. R., & Bauman, J. E. (2016). The STAT3 pathway as a therapeutic target in head and neck cancer: Barriers and innovations. *Oral Oncology*, *56*, 84–92. https://doi.org/10.1016/j.oraloncology.2015.11.022

Gong, X.-M., Li, Y.-F., Luo, J., Wang, J.-Q., Wei, J., Wang, J.-Q., Xiao, T., Xie, C., Hong, J., Ning, G., Shi, X.-J., Li, B.-L., Qi, W., & Song, B.-L. (2019). Gpnmb secreted from liver promotes lipogenesis in white adipose tissue and aggravates obesity and insulin resistance. *Nature Metabolism*, *1*(5), 570–583. https://doi.org/10.1038/s42255-019-0065-4

Han, J., Fujisawa, T., Husain, S. R., & Puri, R. K. (2014). Identification and characterization of cancer stem cells in human head and neck squamous cell carcinoma. *BMC Cancer*, *14*(1), 173. https://doi.org/10.1186/1471-2407-14-173

Hanemaaijer, S. H., van Gijn, S. E., Oosting, S. F., Plaat, B. E. C., Moek, K. L., Schuuring, E. M., van der Laan, B. F. A. M., Roodenburg, J. L. N., van Vugt, M. A. T. M., van der Vegt, B., & Fehrmann, R. S. N. (2018). Data-Driven prioritisation of antibody-drug conjugate targets in head and neck squamous cell carcinoma. *Oral Oncology*, *80*, 33–39. https://doi.org/10.1016/j.oraloncology.2018.03.005

Hannigan, A., Smith, P., Kalna, G., Lo Nigro, C., Orange, C., O'Brien, D. I., Shah, R., Syed, N., Spender, L. C., Herrera, B., Thurlow, J. K., Lattanzio, L., Monteverde, M., Maurer, M. E., Buffa, F. M., Mann, J., Chu, D. C. K., West, C. M. L., Patridge, M., … Inman, G. J. (2010). Epigenetic downregulation of human disabled homolog 2 switches TGF-beta from a tumor suppressor to a tumor promoter. *The Journal of Clinical Investigation*, *120*(8), 2842–2857. https://doi.org/10.1172/JCI36125

Herchenhorn, D., & Ferreira, C. G. (2011). Targeting Epidermal Growth Factor Receptor to

Optimize Chemoradiotherapy in Locally Advanced Head and Neck Cancer: Has Biology Been Taken Into Account? *Journal of Clinical Oncology*, *29*(10), e283–e284. https://doi.org/10.1200/JCO.2010.33.8087

Hood, J. D., & Cheresh, D. A. (2002). Role of integrins in cell invasion and migration. *Nature Reviews Cancer*, *2*(2), 91–100. https://doi.org/10.1038/nrc727

Hoover, D. M., Rajashankar, K. R., Blumenthal, R., Puri, A., Oppenheim, J. J., Chertov, O., & Lubkowski, J. (2000). The Structure of Human β-Defensin-2 Shows Evidence of Higher Order Oligomerization. *Journal of Biological Chemistry*, *275*(42), 32911–32918. https://doi.org/10.1074/jbc.M006098200

Hudson, A. L., Parker, N. R., Khong, P., Parkinson, J. F., Dwight, T., Ikin, R. J., Zhu, Y., Chen, J., Wheeler, H. R., & Howell, V. M. (2018). Glioblastoma Recurrence Correlates With Increased APE1 and Polarization Toward an Immuno-Suppressive Microenvironment. *Frontiers in Oncology*, *8*. https://doi.org/10.3389/fonc.2018.00314

Hüttenrauch, M., Ogorek, I., Klafki, H., Otto, M., Stadelmann, C., Weggen, S., Wiltfang, J., & Wirths, O. (2018). Glycoprotein NMB: a novel Alzheimer's disease associated marker expressed in a subset of activated microglia. *Acta Neuropathologica Communications*, *6*(1), 108. https://doi.org/10.1186/s40478-018-0612-3

Johnson, D. E., Burtness, B., Leemans, C. R., Lui, V. W. Y., Bauman, J. E., & Grandis, J. R. (2020). Head and neck squamous cell carcinoma. *Nature Reviews. Disease Primers*, *6*(1), 92. https://doi.org/10.1038/s41572-020-00224-3

Joly, S., Compton, L. M., Pujol, C., Kurago, Z. B., & Guthmiller, J. M. (2009). Loss of human β-defensin 1, 2, and 3 expression in oral squamous cell carcinoma. *Oral Microbiology and Immunology*, *24*(5), 353–360. https://doi.org/10.1111/j.1399-302X.2009.00512.x

Kalyankrishna, S., & Grandis, J. R. (2006). Epidermal Growth Factor Receptor Biology in Head and Neck Cancer. *Journal of Clinical Oncology*, *24*(17), 2666–2672. https://doi.org/10.1200/JCO.2005.04.8306

Koeninger, L., Armbruster, N. S., Brinch, K. S., Kjaerulf, S., Andersen, B., Langnau, C., Autenrieth, S. E., Schneidawind, D., Stange, E. F., Malek, N. P., Nordkild, P., Jensen, B. A. H., & Wehkamp, J. (2020). Human β-Defensin 2 Mediated Immune Modulation as Treatment for Experimental Colitis. *Frontiers in Immunology*, *11*. https://doi.org/10.3389/fimmu.2020.00093

Kontić, M., Milovanović, J., Čolović, Z., Poljak, N. K., Šundov, Ž., Sučić, A., & Pešutić-Pisac, V. (2015). Epidermal growth factor receptor (EGFR) expression in patients with laryngeal squamous cell carcinoma. In *European Archives of Oto-Rhino-Laryngology* (Vol. 272, Issue 2, pp. 401–405). https://doi.org/10.1007/s00405-014-3323-9

Kriegs, M., Clauditz, T. S., Hoffer, K., Bartels, J., Buhs, S., Gerull, H., Zech, H. B., Bußmann, L., Struve, N., Rieckmann, T., Petersen, C., Betz, C. S., Rothkamm, K., Nollau, P., & Münscher, A. (2019). Analyzing expression and phosphorylation of the EGF receptor in HNSCC. *Scientific Reports*, *9*(1), 13564. https://doi.org/10.1038/s41598-019-49885-5

Krishnamurthy, S., & Nör, J. E. (2012). Head and Neck Cancer Stem Cells. *Journal of Dental Research*, *91*(4), 334–340. https://doi.org/10.1177/0022034511423393

Kuper, H., Adami, H.-O., & Boffetta, P. (2002). Tobacco use, cancer causation and public health impact. *Journal of Internal Medicine*, *251*(6), 455–466. https://doi.org/10.1046/j.1365-2796.2002.00993.x

Lavertu, P., Adelstein, D. J., Myles, J., & Secic, M. (2001). P53 and Ki-67 as outcome predictors for advanced squamous cell cancers of the head and neck treated with chemoradiotherapy.

The Laryngoscope, *111*(11 Pt 1), 1878–1892. https://doi.org/10.1097/00005537-200111000-00002

Lee, J., Park, M., Ko, Y., Kim, B., Kim, O., Hyun, H., Kim, D., Sohn, H., Moon, Y. L., & Lim, W. (2017). Ectopic overexpression of CD133 in HNSCC makes it resistant to commonly used chemotherapeutics. *Tumor Biology*, *39*(4), 101042831769553. https://doi.org/10.1177/1010428317695534

Lee, S. H., Oh, S.-Y., Do, S. I., Lee, H. J., Kang, H. J., Rho, Y. S., Bae, W. J., & Lim, Y. C. (2014). SOX2 regulates self-renewal and tumorigenicity of stem-like cells of head and neck squamous cell carcinoma. *British Journal of Cancer*, *111*(11), 2122–2130. https://doi.org/10.1038/bjc.2014.528

Leemans, C. R., Braakhuis, B. J. M., & Brakenhoff, R. H. (2011). The molecular biology of head and neck cancer. *Nature Reviews Cancer*, *11*(1), 9–22. https://doi.org/10.1038/nrc2982

Lefebvre, J. L., Pointreau, Y., Rolland, F., Alfonsi, M., Baudoux, A., Sire, C., de Raucourt, D., Malard, O., Degardin, M., Tuchais, C., Blot, E., Rives, M., Reyt, E., Tourani, J. M., Geoffrois, L., Peyrade, F., Guichard, F., Chevalier, D., Babin, E., … Bardet, E. (2013). Induction Chemotherapy Followed by Either Chemoradiotherapy or Bioradiotherapy for Larynx Preservation: The TREMPLIN Randomized Phase II Study. *Journal of Clinical Oncology*, *31*(7), 853–859. https://doi.org/10.1200/JCO.2012.42.3988

Li, H., Xiao, Y., Wu, C.-C., Yang, L.-L., Cao, L.-Y., Chen, D.-R., Zhou, J.-J., Zhang, W.-F., & Sun, Z.-J. (2019). High expression of GPNMB predicts poor prognosis in head and neck squamous cell carcinoma. *Histology and Histopathology*, *34*(7), 803–810. https://doi.org/10.14670/HH-18-084

Liguori, M., Digifico, E., Vacchini, A., Avigni, R., Colombo, F. S., Borroni, E. M., Farina, F.

M., Milanesi, S., Castagna, A., Mannarino, L., Craparotta, I., Marchini, S., Erba, E., Panini, N., Tamborini, M., Rimoldi, V., Allavena, P., & Belgiovine, C. (2021). The soluble glycoprotein NMB (GPNMB) produced by macrophages induces cancer stemness and metastasis via CD44 and IL-33. *Cellular & Molecular Immunology*, *18*(3), 711–722. https://doi.org/10.1038/s41423-020-0501-0

Machiels, J.-P., René Leemans, C., Golusinski, W., Grau, C., Licitra, L., & Gregoire, V. (2020). Squamous cell carcinoma of the oral cavity, larynx, oropharynx and hypopharynx: EHNS–ESMO–ESTRO Clinical Practice Guidelines for diagnosis, treatment and follow-up. *Annals of Oncology*, *31*(11), 1462–1475. https://doi.org/10.1016/j.annonc.2020.07.011

Magrini, S. M., Buglione, M., Corvò, R., Pirtoli, L., Paiar, F., Ponticelli, P., Petrucci, A., Bacigalupo, A., Crociani, M., Lastrucci, L., Vecchio, S., Bonomo, P., Pasinetti, N., Triggiani, L., Cavagnini, R., Costa, L., Tonoli, S., Maddalo, M., & Grisanti, S. (2016). Cetuximab and Radiotherapy Versus Cisplatin and Radiotherapy for Locally Advanced Head and Neck Cancer: A Randomized Phase II Trial. *Journal of Clinical Oncology*, *34*(5), 427–435. https://doi.org/10.1200/JCO.2015.63.1671

Major, A. G., Pitty, L. P., & Farah, C. S. (2013). Cancer Stem Cell Markers in Head and Neck Squamous Cell Carcinoma. *Stem Cells International*, *2013*, 1–13. https://doi.org/10.1155/2013/319489

Maric, G., Annis, M. G., MacDonald, P. A., Russo, C., Perkins, D., Siwak, D. R., Mills, G. B., & Siegel, P. M. (2019). GPNMB augments Wnt-1 mediated breast tumor initiation and growth by enhancing PI3K/AKT/mTOR pathway signaling and β-catenin activity. *Oncogene*, *38*(26), 5294–5307. https://doi.org/10.1038/s41388-019-0793-7

Maric, G., Rose, A. A., Annis, M. G., & Siegel, P. M. (2013). Glycoprotein non-metastatic b

(GPNMB): A metastatic mediator and emerging therapeutic target in cancer. *OncoTargets and Therapy*, *6*, 839–852. https://doi.org/10.2147/OTT.S44906

Meng, P., & Ghosh, R. (2014). Transcription addiction: can we garner the Yin and Yang functions of E2F1 for cancer therapy? *Cell Death & Disease*, *5*(8), e1360–e1360. https://doi.org/10.1038/cddis.2014.326

Moore, N., & Lyle, S. (2011). Quiescent, Slow-Cycling Stem Cell Populations in Cancer: A Review of the Evidence and Discussion of Significance. *Journal of Oncology*, *2011*, 1–11. https://doi.org/10.1155/2011/396076

Nagy, Á., Munkácsy, G., & Győrffy, B. (2021). Pancancer survival analysis of cancer hallmark genes. *Scientific Reports*, *11*(1), 6047. https://doi.org/10.1038/s41598-021-84787-5

Najafi, M., Farhood, B., & Mortezaee, K. (2019). Cancer stem cells (CSCs) in cancer progression and therapy. *Journal of Cellular Physiology*, *234*(6), 8381–8395. https://doi.org/10.1002/jcp.27740

Nowak, K. (2006). BMI1 is a target gene of E2F-1 and is strongly expressed in primary neuroblastomas. *Nucleic Acids Research*, *34*(6), 1745–1754. https://doi.org/10.1093/nar/gkl119

O'Brien, C. A., Pollett, A., Gallinger, S., & Dick, J. E. (2007). A human colon cancer cell capable of initiating tumour growth in immunodeficient mice. *Nature*, *445*(7123), 106–110. https://doi.org/10.1038/nature05372

Okita, Y., Kimura, M., Xie, R., Chen, C., Shen, L. T.-W., Kojima, Y., Suzuki, H., Muratani, M., Saitoh, M., Semba, K., Heldin, C.-H., & Kato, M. (2017). The transcription factor MAFK induces EMT and malignant progression of triple-negative breast cancer cells through its target GPNMB. *Science Signaling*, *10*(474), eaak9397.

https://doi.org/10.1126/scisignal.aak9397

Ono, Y., Chiba, S., Yano, H., Nakayama, N., Saio, M., Tsuruma, K., Shimazawa, M., Iwama, T., & Hara, H. (2016). Glycoprotein nonmetastatic melanoma protein B (GPNMB) promotes the progression of brain glioblastoma via Na+/K+-ATPase. *Biochemical and Biophysical Research Communications*, *481*(1–2), 7–12. https://doi.org/10.1016/j.bbrc.2016.11.034

Oshimori, N., Oristian, D., & Fuchs, E. (2015). TGF-β promotes heterogeneity and drug resistance in squamous cell carcinoma. *Cell*, *160*(5), 963–976. https://doi.org/10.1016/j.cell.2015.01.043

Paget-Bailly, S., Cyr, D., & Luce, D. (2012). Occupational Exposures and Cancer of the Larynx—Systematic Review and Meta-analysis. *Journal of Occupational & Environmental Medicine*, *54*(1), 71–84. https://doi.org/10.1097/JOM.0b013e31823c1343

Perdomo, S., Anantharaman, D., Foll, M., Abedi-Ardekani, B., Durand, G., Reis Rosa, L. A., Holmila, R., Le Calvez-Kelm, F., Tajara, E. H., Wünsch-Filho, V., Levi, J. E., Vilensky, M., Polesel, J., Holcatova, I., Simonato, L., Canova, C., Lagiou, P., McKay, J. D., & Brennan, P. (2018). Genomic analysis of head and neck cancer cases from two high incidence regions. *PLOS ONE*, *13*(1), e0191701. https://doi.org/10.1371/journal.pone.0191701

Poeta, M. L., Manola, J., Goldwasser, M. A., Forastiere, A., Benoit, N., Califano, J. A., Ridge, J. A., Goodwin, J., Kenady, D., Saunders, J., Westra, W., Sidransky, D., & Koch, W. M. (2007). TP53 Mutations and Survival in Squamous-Cell Carcinoma of the Head and Neck. *New England Journal of Medicine*, *357*(25), 2552–2561. https://doi.org/10.1056/NEJMoa073770

Pulte, D., & Brenner, H. (2010). Changes in Survival in Head and Neck Cancers in the Late 20th

and Early 21st Century: A Period Analysis. *The Oncologist*, *15*(9), 994–1001. https://doi.org/10.1634/theoncologist.2009-0289

Radecki, D. Z., Wang, A. R., Johnson, A. S., Overman, C. A., Thatcher, M. M., Iyer, G., & Samanta, J. (2021). Gpnmb inhibits oligodendrocyte differentiation of adult neural stem cells by amplifying TGFβ1 signaling. *BioRxiv*. https://doi.org/10.1101/2021.08.13.456269

Ricci-Vitiani, L., Lombardi, D. G., Pilozzi, E., Biffoni, M., Todaro, M., Peschle, C., & De Maria, R. (2007). Identification and expansion of human colon-cancer-initiating cells. *Nature*, *445*(7123), 111–115. https://doi.org/10.1038/nature05384

Rivelli, T. G., Mak, M. P., Martins, R. E., da Costa e Silva, V. T., & de Castro, G. (2014). Cisplatin based chemoradiation late toxicities in head and neck squamous cell carcinoma patients. *Discovery Medicine*, *20*(108), 57–66. https://doi.org/10.1016/j.bbrc.2014.09.021

Rivelli, T. G., Mak, M. P., Martins, R. E., da Costa e Silva, V. T., & de Castro, G. (2015). Cisplatin based chemoradiation late toxicities in head and neck squamous cell carcinoma patients. *Discovery Medicine*, *20*(108), 57–66. http://www.ncbi.nlm.nih.gov/pubmed/26321088

Rizqiawan, A., Tobiume, K., Okui, G., Yamamoto, K., Shigeishi, H., Ono, S., Shimasue, H., Takechi, M., Higashikawa, K., & Kamata, N. (2013). Autocrine galectin-1 promotes collective cell migration of squamous cell carcinoma cells through up-regulation of distinct integrins. *Biochemical and Biophysical Research Communications*, *441*(4), 904–910. https://doi.org/10.1016/j.bbrc.2013.10.152

Rose, A. A. N., Annis, M. G., Dong, Z., Pepin, F., Hallett, M., Park, M., & Siegel, P. M. (2010). ADAM10 Releases a Soluble Form of the GPNMB/Osteoactivin Extracellular Domain with Angiogenic Properties. *PLoS ONE*, *5*(8), e12093.

https://doi.org/10.1371/journal.pone.0012093

Rose, A. A. N., Annis, M. G., Frederick, D. T., Biondini, M., Dong, Z., Kwong, L., Chin, L., Keler, T., Hawthorne, T., Watson, I. R., Flaherty, K. T., & Siegel, P. M. (2016). MAPK Pathway Inhibitors Sensitize BRAF-Mutant Melanoma to an Antibody-Drug Conjugate Targeting GPNMB. *Clinical Cancer Research*, *22*(24), 6088–6098. https://doi.org/10.1158/1078-0432.CCR-16-1192

Schrader, C., Janssen, D., Klapper, W., Siebmann, J.-U., Meusers, P., Brittinger, G., Kneba, M., Tiemann, M., & Parwaresch, R. (2005). Minichromosome maintenance protein 6, a proliferation marker superior to Ki-67 and independent predictor of survival in patients with mantle cell lymphoma. *British Journal of Cancer*, *93*(8), 939–945. https://doi.org/10.1038/sj.bjc.6602795

Shah, P. A., Huang, C., Li, Q., Kazi, S. A., Byers, L. A., Wang, J., Johnson, F. M., & Frederick, M. J. (2020). NOTCH1 Signaling in Head and Neck Squamous Cell Carcinoma. *Cells*, *9*(12), 2677. https://doi.org/10.3390/cells9122677

Sheng, M. H.-C., Wergedal, J. E., Mohan, S., & Lau, K.-H. W. (2008). Osteoactivin is a novel osteoclastic protein and plays a key role in osteoclast differentiation and activity. *FEBS Letters*, *582*(10), 1451–1458. https://doi.org/10.1016/j.febslet.2008.03.030

Shi, N., Jin, F., Zhang, X., Clinton, S. K., Pan, Z., & Chen, T. (2014). Overexpression of human β-defensin 2 promotes growth and invasion during esophageal carcinogenesis. *Oncotarget*, *5*(22), 11333–11344. https://doi.org/10.18632/oncotarget.2416

Shikano, S., Bonkobara, M., Zukas, P. K., & Ariizumi, K. (2001). Molecular Cloning of a Dendritic Cell-associated Transmembrane Protein, DC-HIL, That Promotes RGD-dependent Adhesion of Endothelial Cells through Recognition of Heparan Sulfate

Proteoglycans. *Journal of Biological Chemistry*, *276*(11), 8125–8134. https://doi.org/10.1074/jbc.M008539200

Siegel, R. L., Miller, K. D., & Jemal, A. (2016). Cancer statistics, 2016. *CA: A Cancer Journal for Clinicians*, *66*(1), 7–30. https://doi.org/10.3322/caac.21332

Silva, S. D., Agostini, M., Nishimoto, I. N., Coletta, R. D., Alves, F. A., Lopes, M. A., Kowalski, L. P., & Graner, E. (2004). Expression of fatty acid synthase, ErbB2 and Ki-67 in head and neck squamous cell carcinoma. A clinicopathological study. *Oral Oncology*, *40*(7), 688–696. https://doi.org/10.1016/j.oraloncology.2004.01.004

Singh, S. K., Hawkins, C., Clarke, I. D., Squire, J. A., Bayani, J., Hide, T., Henkelman, R. M., Cusimano, M. D., & Dirks, P. B. (2004). Identification of human brain tumour initiating cells. *Nature*, *432*(7015), 396–401. https://doi.org/10.1038/nature03128

Sittel, C., Eckel, H. E., Damm, M., von Pritzbuer, E., & Kvasnicka, H. M. (2000). Ki-67 (MIB1), p53, and Lewis-X (LeuM1) as prognostic factors of recurrence in T1 and T2 laryngeal carcinoma. *The Laryngoscope*, *110*(6), 1012–1017. https://doi.org/10.1097/00005537-200006000-00024

Soliman, N. A., & Yussif, S. M. (2016). Ki-67 as a prognostic marker according to breast cancer molecular subtype. *Cancer Biology & Medicine*, *13*(4), 496–504. https://doi.org/10.20892/j.issn.2095-3941.2016.0066

Specenier, P., & Vermorken, J. B. (2011). Cetuximab in the treatment of squamous cell carcinoma of the head and neck. *Expert Review of Anticancer Therapy*, *11*(4), 511–524. https://doi.org/10.1586/era.11.20

Steuer, C. E., El-Deiry, M., Parks, J. R., Higgins, K. A., & Saba, N. F. (2017). An update on larynx cancer. *CA: A Cancer Journal for Clinicians*, *67*(1), 31–50.

https://doi.org/10.3322/caac.21386

Stransky, N., Egloff, A. M., Tward, A. D., Kostic, A. D., Cibulskis, K., Sivachenko, A., Kryukov, G. V., Lawrence, M. S., Sougnez, C., McKenna, A., Shefler, E., Ramos, A. H., Stojanov, P., Carter, S. L., Voet, D., Cortés, M. L., Auclair, D., Berger, M. F., Saksena, G., … Grandis, J. R. (2011). The Mutational Landscape of Head and Neck Squamous Cell Carcinoma. *Science*, *333*(6046), 1157–1160. https://doi.org/10.1126/science.1208130

Sun, S., Wu, Y., Guo, W., Yu, F., Kong, L., Ren, Y., Wang, Y., Yao, X., Jing, C., Zhang, C., Liu, M., Zhang, Y., Zhao, M., Li, Z., Wu, C., Qiao, Y., Yang, J., Wang, X., Zhang, L., … Zhou, X. (2018). STAT3/HOTAIR Signaling Axis Regulates HNSCC Growth in an EZH2-dependent Manner. *Clinical Cancer Research*, *24*(11), 2665–2677. https://doi.org/10.1158/1078-0432.CCR-16-2248

Talamini, R., Bosetti, C., La Vecchia, C., Dal Maso, L., Levi, F., Bidoli, E., Negri, E., Pasche, C., Vaccarella, S., Barzan, L., & Franceschi, S. (2002). Combined effect of tobacco and alcohol on laryngeal cancer risk: a case-control study. *Cancer Causes & Control : CCC*, *13*(10), 957–964. https://doi.org/10.1023/a:1021944123914

Tomihari, M., Chung, J.-S., Akiyoshi, H., Cruz, P. D., & Ariizumi, K. (2010). DC-HIL/Glycoprotein Nmb Promotes Growth of Melanoma in Mice by Inhibiting the Activation of Tumor-Reactive T Cells. *Cancer Research*, *70*(14), 5778–5787. https://doi.org/10.1158/0008-5472.CAN-09-2538

Uckun, F. M., Sather, H., Reaman, G., Shuster, J., Land, V., Trigg, M., Gunther, R., Chelstrom, L., Bleyer, A., & Gaynon, P. (1995). Leukemic cell growth in SCID mice as a predictor of relapse in high-risk B-lineage acute lymphoblastic leukemia. *Blood*, *85*(4), 873–878. http://www.ncbi.nlm.nih.gov/pubmed/7849309

van Schaik, J. E., Hanemaaijer, S. H., Halmos, G. B., Witjes, M. J. H., van der Laan, B. F. A. M., van der Vegt, B., & Plaat, B. E. C. (2020). Glycoprotein Nonmetastatic Melanoma Protein B as Potential Imaging Marker in Posttherapeutic Metastatic Head and Neck Cancer. *Otolaryngology - Head and Neck Surgery (United States)*, *163*(6), 1202–1208. https://doi.org/10.1177/0194599820932869

Vermorken, J. B., Mesia, R., Rivera, F., Remenar, E., Kawecki, A., Rottey, S., Erfan, J., Zabolotnyy, D., Kienzer, H.-R., Cupissol, D., Peyrade, F., Benasso, M., Vynnychenko, I., De Raucourt, D., Bokemeyer, C., Schueler, A., Amellal, N., & Hitt, R. (2008). Platinum-Based Chemotherapy plus Cetuximab in Head and Neck Cancer. *New England Journal of Medicine*, *359*(11), 1116–1127. https://doi.org/10.1056/NEJMoa0802656

Walcher, L., Kistenmacher, A.-K., Suo, H., Kitte, R., Dluczek, S., Strauß, A., Blaudszun, A.-R., Yevsa, T., Fricke, S., & Kossatz-Boehlert, U. (2020). Cancer Stem Cells—Origins and Biomarkers: Perspectives for Targeted Personalized Therapies. *Frontiers in Immunology*, *11*. https://doi.org/10.3389/fimmu.2020.01280

Wang, C., Okita, Y., Zheng, L., Shinkai, Y., Manevich, L., Chin, J. M., Kimura, T., Suzuki, H., Kumagai, Y., & Kato, M. (2021). Glycoprotein NMB functions with growth factor signaling to induce tumorigenesis through its serine phosphorylation. *Cancer Science*, *February*, 1–11. https://doi.org/10.1111/cas.15090

Wang, J., Xi, L., Gooding, W., Godfrey, T. E., & Ferris, R. L. (2004). Chemokine Receptors 6 and 7 Identify a Metastatic Expression Pattern in Squamous Cell Carcinoma of the Head and Neck. In *Current Research in Head and Neck Cancer* (pp. 121–133). KARGER. https://doi.org/10.1159/000082501

Wang, T., Shigdar, S., Gantier, M. P., Hou, Y., Wang, L., Li, Y., Shamaileh, H. Al, Yin, W.,

Zhou, S.-F., Zhao, X., & Duan, W. (2015). Cancer stem cell targeted therapy: progress amid controversies. *Oncotarget*, *6*(42), 44191–44206. https://doi.org/10.18632/oncotarget.6176

Wang, Y., & Tatakis, D. (2018). Smoking alters the normal transcriptome of healthy human gingiva. *Tobacco Induced Diseases*, *16*(3). https://doi.org/10.18332/tid/94762

Wu, Q., Wang, D., Zhang, Z., Wang, Y., Yu, W., Sun, K., Maimela, N., Sun, Z., Liu, J., Yuan, W., & Zhang, Y. (2020). DEFB4A is a potential prognostic biomarker for colorectal cancer. *Oncology Letters*, *20*(4), 1–1. https://doi.org/10.3892/ol.2020.11975

Xiao, M., Liu, L., Zhang, S., Yang, X., & Wang, Y. (2018). Cancer stem cell biomarkers for head and neck squamous cell carcinoma: A bioinformatic analysis. *Oncology Reports*. https://doi.org/10.3892/or.2018.6771

Xie, R., Okita, Y., Ichikawa, Y., Fikry, M. A., Huynh Dam, K. T., Tran, S. T. P. D., & Kato, M. (2019). Role of the kringle-like domain in glycoprotein NMB for its tumorigenic potential. *Cancer Science*, *110*(7), 2237–2246. https://doi.org/10.1111/cas.14076

Yang, L., Shi, P., Zhao, G., Xu, J., Peng, W., Zhang, J., Zhang, G., Wang, X., Dong, Z., Chen, F., & Cui, H. (2020). Targeting cancer stem cell pathways for cancer therapy. *Signal Transduction and Targeted Therapy*, *5*(1), 8. https://doi.org/10.1038/s41392-020-0110-5

Yu, F., Sim, A. C. N., Li, C., Li, Y., Zhao, X., Wang, D.-Y., & Loh, K. S. (2013). Identification of a subpopulation of nasopharyngeal carcinoma cells with cancer stem-like cell properties by high aldehyde dehydrogenase activity. *The Laryngoscope*, *123*(8), 1903–1911. https://doi.org/10.1002/lary.24003

Zhang, J., Lin, H., Jiang, H., Jiang, H., Xie, T., Wang, B., Huang, X., Lin, J., Xu, A., Li, R., Zhang, J., & Yuan, Y. (2020). A key genomic signature associated with lymphovascular invasion in head and neck squamous cell carcinoma. *BMC Cancer*, *20*(1), 266.

https://doi.org/10.1186/s12885-020-06728-1

Zhang, M., Deng, W., Gong, H., Li, C., Wang, Y., Liu, X., Tao, L., & Zhou, L. (2019). Clinical effect of postoperative chemoradiotherapy in resected advanced laryngeal squamous cell carcinoma. *Oncology Letters*. https://doi.org/10.3892/ol.2019.10104

Zhang, P., Liu, W., Zhu, C., Yuan, X., Li, D., Gu, W., Ma, H., Xie, X., & Gao, T. (2012). Silencing of GPNMB by siRNA Inhibits the Formation of Melanosomes in Melanocytes in a MITF-Independent Fashion. *PLoS ONE*, *7*(8), e42955. https://doi.org/10.1371/journal.pone.0042955

Zhou, Y., Zhou, B., Pache, L., Chang, M., Khodabakhshi, A. H., Tanaseichuk, O., Benner, C., & Chanda, S. K. (2019). Metascape provides a biologist-oriented resource for the analysis of systems-level datasets. *Nature Communications*, *10*(1), 1523. https://doi.org/10.1038/s41467-019-09234-6

ACKNOWLEDGEMENTS

I would like to express my deepest gratitude and respect to my supervisor, Professor Mitsuyasu Kato for accepting me into Experimental Pathology laboratory and giving me the opportunity to experience the life within science as a PhD-student. Professor's wise leadership, profound knowledge in oncology and experimental techniques helped me to adjust in the new environment, to evolve my scientific thinking, and successfully pass steps of the Doctoral Program course. Thanks to him, I could be a part of this well-managed, mutually beneficial, and friendly partnership.

I am beyond grateful to my sub-supervisor assistant Professor Yukari Okita for the direct and explicit help with my work in this laboratory. I cannot imagine the step-by-step successful progress without her contribution. With her supervision and necessary assistance I could obtain new skills in laboratory techniques and in manuscript writing – necessary aspects of the study in science and future carrier growth. And all of this was inseverable with her personal kindness and deep care.

Big thanks to assistant Professor Yukihide Watanabe for his daily support, helpful suggestions, and personal involvement in my study and work within Experimental Pathology laboratory. I am also grateful to all laboratory members and co-authors of the manuscript for their theoretical guidance, practical contributions, and personal support within and beyond the workspace. All of them made my life in Japan rich and unforgettably happy.

My sincere regards and thanks to assistant Professor Takehito Sugasawa from Laboratory of Sports Medicine. Before the start of my PhD life he was the first, who introduced me to the field of science and gifted me the interest in science generally. His explicit help, fresh look to my project

and important suggestions could enrich my work with novelty, while above that, he became my close friend.

My deepest gratitude for all members of the Department of Otolaryngology in University of Tsukuba, personally to Professor Keiji Tabuchi and Dr. Yasuhito Okano for the great clinical impact into my work. This collaboration and critically important guidance from Dr. Okano gave me a great experience and best results during my education.

I am very grateful to my teacher Dr. Bryan Mathis for his big support in my study and in elaboration of my writing skills. With his help I could not only benefit from my work, but also enjoy the experience of PhD life.

I thank the MEXT organization for their crucial financial support throughout my study and life in Japan. Thanks to the taxpayers in Japan and invested grants, I could continue and finish my research, providing a determined impact into science worldwide.

In this section I sincerely thank all of my friends, who directly and indirectly supported me during the PhD-experience and general life in Japan. I would like to express my profound gratitude to my teacher and friend Ms. Kikue Sato and to my girlfriend Haruna Ueda for their altruistic help and disparate care.

My final and deepest thankfulness I would like to dedicate to my beloved family, mother Rina and father Igor, for their sincere daily support. I cannot thank enough their help and care they are continuously giving me, while being abroad. You are in my heart.